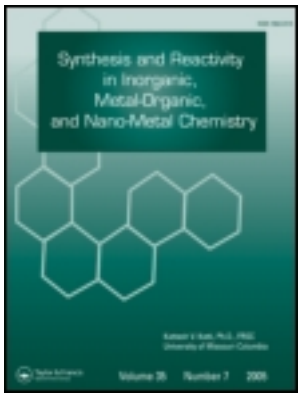

Synthesis and Reactivity in Inorganic, Metal-Organic, and Nano-Metal Chemistry

Publication details, including instructions for authors and subscription information:
http://www.tandfonline.com/loi/lsrt20

Recent Advances in Application of Polyoxometalates for the Synthesis of Nanoparticles

Fatemeh F. Bamoharram [a], Ali Ahmadpour [b], Majid M. Heravi [c], Ali Ayati [b], Hamed Rashidi [b] & Bahareh Tanhaei [b]

[a] Department of Chemistry, Mashhad Branch, Islamic Azad University, Mashhad, I. R. Iran

[b] Department of Chemical Engineering, Ferdowsi University of Mashhad, Mashhad, I. R. Iran

[c] Department of Chemistry, School of Sciences, Alzahra University, Tehran, I. R. Iran

Version of record first published: 23 Mar 2012

To cite this article: Fatemeh F. Bamoharram, Ali Ahmadpour, Majid M. Heravi, Ali Ayati, Hamed Rashidi & Bahareh Tanhaei (2012): Recent Advances in Application of Polyoxometalates for the Synthesis of Nanoparticles, Synthesis and Reactivity in Inorganic, Metal-Organic, and Nano-Metal Chemistry, 42:2, 209-230

To link to this article: http://dx.doi.org/10.1080/15533174.2011.609849

Synthesis and Reactivity in Inorganic, Metal-Organic, and Nano-Metal Chemistry, 42:209–230, 2012

ISSN: 1553-3174 print / 1553-3182 online
DOI: 10.1080/15533174.2011.609849

Taylor & Francis
Taylor & Francis Group

Recent Advances in Application of Polyoxometalates for the Synthesis of Nanoparticles

Fatemeh F. Bamoharram,[1] Ali Ahmadpour,[2] Majid M. Heravi,[3] Ali Ayati,[2] Hamed Rashidi,[2] and Bahareh Tanhaei[2]

[1]*Department of Chemistry, Mashhad Branch, Islamic Azad University, Mashhad, I. R. Iran*
[2]*Department of Chemical Engineering, Ferdowsi University of Mashhad, Mashhad, I. R. Iran*
[3]*Department of Chemistry, School of Sciences, Alzahra University, Tehran, I. R. Iran*

Recent developments in the synthesis of nanoparticles using polyoxometalates (POMs) are reviewed. This review demonstrates the importance and various roles of POMs in developing of nanotechnology. Special attention has been paid to the synthesis of silver, gold, selenium, cadmium sulfide, palladium, and calcium carbonate nanoparticles using POMs.

Keywords nanoparticles, polyoxometalates, silver nanoparticle, synthesis

INTRODUCTION

Interest in nanoparticles (NPs), which are defined as particles with diameters ranging from a few to 100 nm, is rapidly increasing because NPs have unprecedented chemical and physical properties that differ markedly from those of the bulk material.[1] NPs have various applications in electronics,[2] catalysts,[3,4] drug carriers[5,6] and medical devices,[7] sensors,[8] pigments,[9] and magnetic and optical materials.[1]

So far, various methods have been reported on the synthesis of NPs including chemical reduction, [10–12] photochemical reduction,[13,14] radiolytic,[15] electrochemical,[16] and sonochemical methods[17,18] by using various reagents. Most of these methods are expensive and the applications of them cause some drawbacks such as environmental problems, long reaction times, and tedious work-up procedure.

Green chemistry has been defined as a set of principles that reduces or eliminates the use or generation of hazardous substances throughout the entire life of chemical materials.[19,20] Along this line, the green synthesis of NPs involves three main steps, which must be evaluated based on green chemistry perspectives, including (a) selection of solvent medium, (b) selection of environmentally benign reducing agent, and (c) selection of nontoxic substances for the NPs stability.[21]

Polyoxometalates (POMs) have been introduced as promising candidates as green materials. POMs are green and harmless to the environment with respect to corrosiveness, safety, quantity of waste, and separability. Other key green aspects of solid POMs are related to their synthesis in an aqueous process and achievements of successful practical applications. Thus, several novel and facile methods have been proposed to synthesize NPs using POMs to serve as reducing reagents, photocatalysts, and stabilizers.

Several properties of the present POMs designate them as suitable reagents for the synthesis of nanoparticles with many advantages: (a) it is possible to synthesize them in the reduced form, (b) they are highly soluble in water and are anticipated to do so in non-aqueous solvents upon syntheses with appropriate counter cations (these two features are not usually available with most chemical reductants), (c) the reduced and oxidized forms are simultaneously stable in a large pH domain (provisionally, these forms must be noted to be insensitive to dioxygen, a feature that might be useful, at the very least for their storage), (d) several of them can be operated in pure water without any additive, (e) their apparent formal potentials can be tuned finely to match that of the metallic cation to be reduced, and (f) finally, they provide simultaneously a reduction and a stabilization abilities.[22–25]

Therefore the role of POMs in nanoscience and their applications continues to attract significant attention, hence the number of publications and patents continues to grow, and new researchers are entering the field.

Encouraged by our recent successes with POMs as green catalysts,[26–106] we have developed our research in field of nanotechnology,[26,28–30,107–111] and studied synthesis and characterization of silica-supported Preyssler nanoparticles and its catalytic activity in various reactions.

Along in our studies, we have found that despite various reviews on POMs, no review concerning POMs in the synthesis of NPs has been presented. In this review, we wish

Received 16 October 2010; accepted 29 July 2011.
Address correspondence to Fatemeh F. Bamoharram, Rahnamaie Street, Rahnamaie 26, Faculty of Science, Department of Chemistry, Mashhad, I. R. Iran, 91735-413. E-mail: fbamoharram@mshdiau.ac.ir

to present recent developments in the synthesis of NPs using POMs.

SILVER NANOPARTICLES

There are different methods reported for the synthesis of silver nanoparticles (Ag NPs).[21] POMs have the potential of synthesizing Ag NPs as well as their applications in recovery of silver.[112] As early as 1956, Chalkley had the inspiration to use photochemically produced, one-electron-reduced Keggin tungstophosphate, $PW_{12}O_{40}{}^{4-}$, to reduce and precipitate silver ions to metallic silver (Equation 1):[113]

$$PW_{1z}O_{4o}^{4-} + Ag^{+} \rightarrow PW_{1z}O_{4o}^{3-} + Ag^{o} \quad [1]$$

The chemical reduction is the most common method for the synthesis of Ag NPs. In general, in the chemical reduction, common reductants are elemental hydrogen, citrate, ascor bate, and borohydride.[114–118] POMs can be reduced in a plethora of ways, for example, photochemically, electrolytically, and with reducing reagents.[22,119,120]

The reduced POMs can act as soluble cathodes, able to reduce several metal ions to the elemental state. The process can be implemented for two basic aims: (a) recovery of valuable or toxic metals that can also be combined with the degradation of organic pollutants in a one-pot system and (b) the synthesis of several metal nanoparticles in a simple and efficient way.[113]

The reduced form of POM, is a powerful reducing reagent, which can be easily reoxidized by a diverse number of chemicals[121] including metal ions (i.e. Ag^{+}, Cu^{2+}, Pd^{2+}, Au^{3+}, Hg^{2+}, or Cr^{6+}).[122]

Troupis et al. suggested a process for reduction of metal ions to their zero state form that takes place in the presence of organic substrates (S; (i.e. alcohols) as electron donors and POMs as photocatalysts in a net photocatalytic cycle, according to the following reactions:[113]

$$POM + S^{h\nu} \rightarrow POM(e^{-}) + S_{OX} \quad [2]$$

$$POM(e^{-}) + M^{n+} \rightarrow POM + M^{0} \quad [3]$$

$$POM(e^{-}) + M^{n+} \rightarrow POM + M^{0}_{coll} \quad [4]$$

In Equation 4 M^{0}_{coll} = colloidal metal. By adjusting the conditions at low ionic strength, synthesis of Ag, Pd, Au, and Pt metal nanoparticles with reasonably small size distribution can be achieved.[113]

Equations 2 and 4 may be separated in time and space (two-pots system), or occur in a one-pot system, where POM plays the double role of photocatalytic reducing reagent and stabilizer. This process takes place within a few seconds at ambient temperature and it can be used for the synthesis of other nanostructured materials, such as bimetallic nanoparticles, nanosheets, or nanorings.[123]

It is noted that by control of the rate of Equation 4, the size of the particles can be controlled. Faster reduction of metal ion leads to smaller and more uniform nanoparticles suggesting that the rate of metal ion reduction affects strongly the initial nucleation of particles.[124] A method for this can be achieved by increasing the concentration of the reducing reagent (reduced POM). Alternatively, the concentration of metal ions also influences the size of the obtained particles, therefore, larger concentrations of metal ions form larger nanoparticles.[28]

Troupis et al. demonstrated that several metal ions, including Ag^{+}, Pd^{2+}, Au^{III}, and Pt^{IV} could form metal nanoparticles in the presence of photochemically reduced Keggin heteropolyanions, such as $[SiW_{12}O_{40}]^{5-}$ and $[PW_{12}O_{40}]^{4-}$ as mild reductants (Figure 1).[25,125]

The volume and negative charge of POMs could account for the prevention of agglomeration of the metal nanoparticles. For example, 12-tungstosilicate considered to be spherical, with a diameter of about 12Å have (4–) negative charge that the anion is not protonated, even at pH = 1.[25] Another benefit of this process is the synthesis of metal nanoparticles is achieved in water as a non-toxic solvent. The TEM pattern of the Ag NPs indicated in Figure 2. It shows the particles are almost spherical with diameter of 15.3 ± 3.4 nm.[25]

Interestingly, selecting POMs (different POMs with increasing negative reduction potential or the same POM with more electrons accumulated on it) having appropriate redox potentials can control the size of Ag nanoparticles. The rates of Ag^{+} reduction parallel the more negative reduction potential for POMs according to the series $H_2W_{12}O_{40}{}^{7-} > SiW_{12}O_{40}{}^{5-} > P_2W_{18}O_{62}{}^{8-} > P_2W_{18}O_{62}{}^{7-} > P_2Mo_{18}O_{62}{}^{10-} > P_2Mo_{18}O_{62}{}^{8-} = 0$.[126] This precise redox-control is summarized in soluble cathode behavior of POMs, which leads to more uniform particles than those obtained with conventional electrochemistry. On the other hand, increasing the concentration of reducing agent (POMs) results in the formation of gradually smaller nanoparticles.[126]

Alternatively, as explained before, the concentration of silver ions influences the size of the particles obtained: increasing the amount of Ag^{+} leads to larger nanoparticles.[126]

Illumination of a system (propan-2-ol/POM/Ag^{+}) with near-visible and UV-light results in synthesis of Ag NPs and Equation 3 changes to:

$$POM^{-} + Ag^{+} \rightarrow POM + Ag^{o}\cdot \quad [5]$$

and S = propan-2-ol.[127]

We have investigated the synthesis of Ag NPs by use of Preyssler acid, $H_{14}[NaP_5W_{30}O_{110}]$, as the reaction promoter, by chemical reduction of silver nitrate in water as an environmentally safe solvent.[109] In this work, Poly(N-vinyl-2-pyrolidone) (PVP) was used as stabilizer, which is an excellent stabilizer to prevent agglomeration through a protection layer on the particles surface and can be readily washed out with acetone/water at the end of reaction.[109,115]

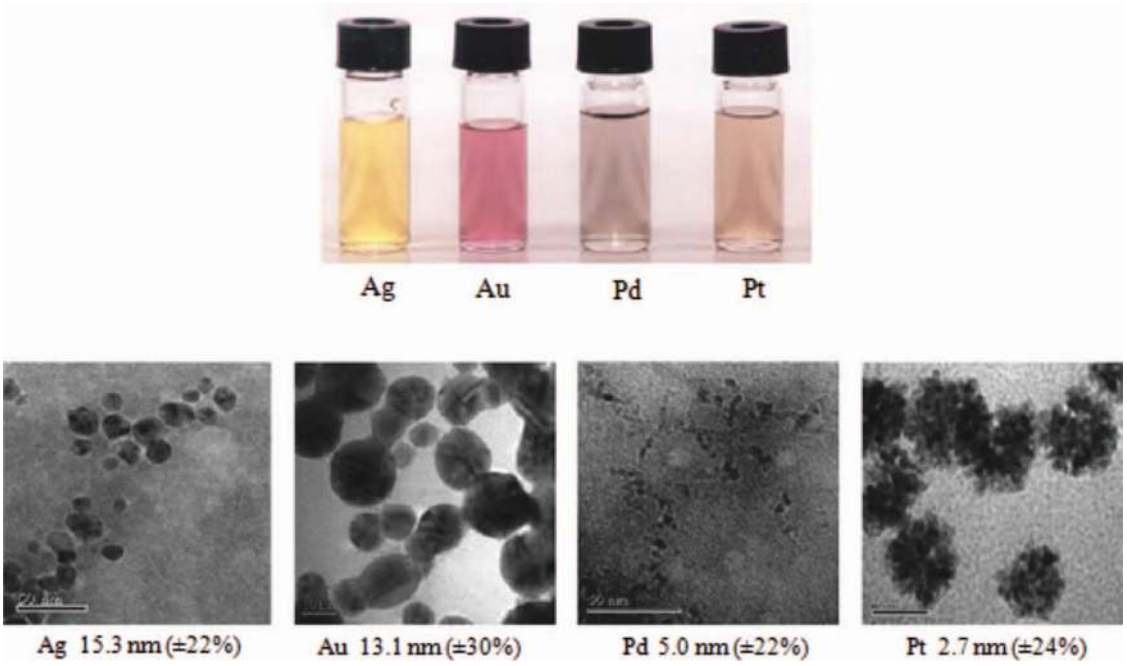

FIG. 1. Color variation (upper part) and TEM graphs of Ag, Au, Pd, and Pt solutions (lower part), obtained upon mixing of photochemically produced, deaerated blue solution of $SiW_{12}O_{40}{}^{5-}$ (3.5×10^{-4} M) with solutions of the corresponding metal ions, $AgNO_3$, $PdCl_2$, H_2PtCl_6 (final concentration 10^{-4} M), or $HAuCl_4$ (final concentration 10^{-3} M), pH 5, T 20°C[113] (color figure available online).

A monitored experiment in the absence of Preyssler has been shown that the formation of nanoparticles is very slow and Preyssler acid is easily kept out after the reaction and will not contaminate the nanosilver particles.[109]

Shanmugam et al.[128] described a single-step chemical route to embed the Ag and Au NPs in composite films. They demonstrated that the silicotungstate ions are necessary for the rapid reduction of metal nanoparticles in composite films in their method. The average particle size of Ag was found to be 16 nm. The particle size can be controlled by dipping time intervals and concentration of metal ion solutions and the particle distribution can be altered by changing the concentration of silicotungstic acid in the composite.[128]

A typical preparation of embedded Ag metal NPs is shown in Figure 3. At first, the composite was synthesized by sol-gel method. After preparation of the gel, it was coated on glass slides by spin coating method. The composite film was dipped into a solution of $AgNO_3$ and then exposed to sunlight. The blue color of the film was gradually changed to yellow within a few minutes, indicating the formation of Ag nanoparticles in

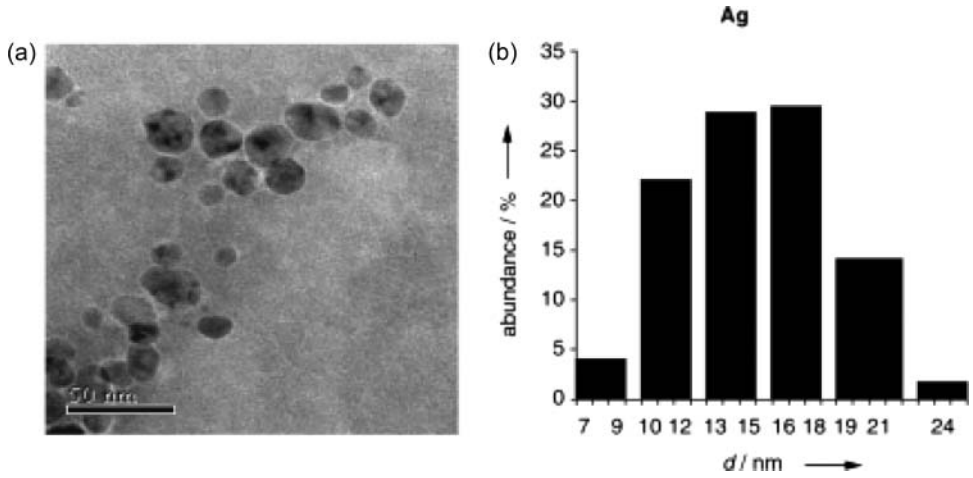

FIG. 2. (a) Transmission electron micrograph and (b) size histogram of the Ag particles.[25]

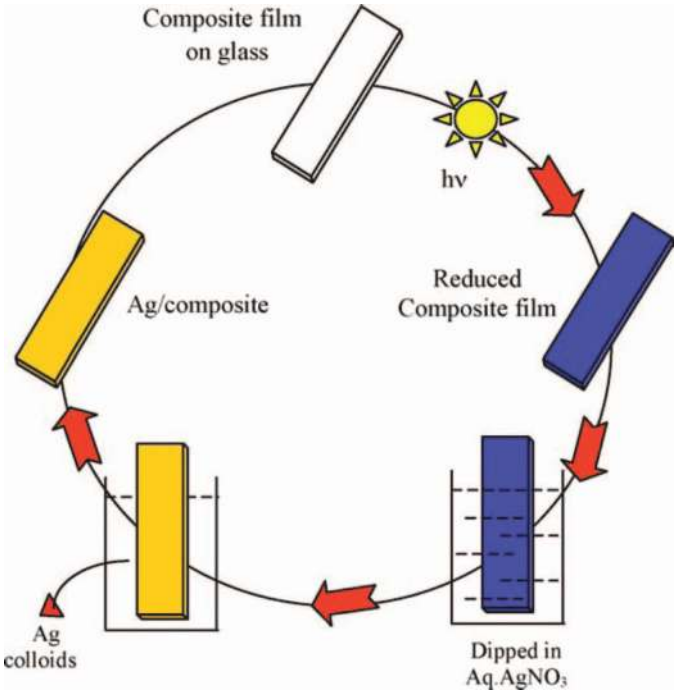

FIG. 3. Preparation of noble metal nanoparticles embedded composite film (color figure available online).[128]

the composite film. The Ag^+ ions from solution diffused inside the film matrix where it is reduced to Ag metal nanoparticles. Figure 4 is shown the TEM image of formations of these Ag NPs in composite film.[128]

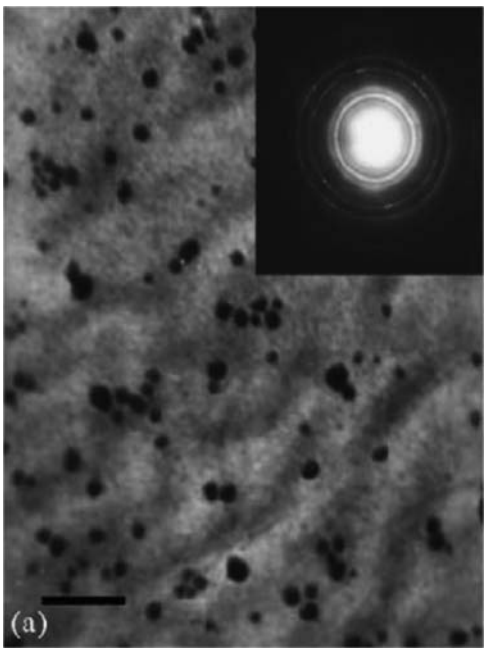

FIG. 4. Transmission electron micrographs of noble Ag nanoparticles embedded composite films. Scale bar 100 nm.

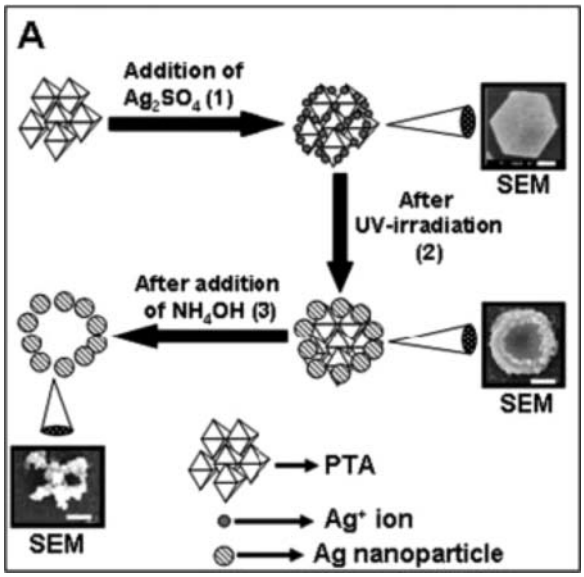

FIG. 5. Scheme illustrating the various steps involved in the phosphotungstate ion-templated synthesis of silver nanoparticles.[129]

The possibility of using the Keggin framework as a UV-switchable reducing matrix is exciting. It has been shown that highly organized assemblies of Ag NPs can be formed by using crystalline Ag^+–Keggin ion colloidal particles as precursors, wherein the Keggin ion host plays the role of a UV-switchable reducing agent.[129]

Figure 5 shows a scheme illustrating the various steps involved in the phosphotungstate ion-templated synthesis of Ag NPs. Crystalline, micron-size colloidal particles of Ag^+ ions complexed with phosphotungstate Keggin ions [$(PW_{12}O_{40})^{3-}$, PTA; step 1, Figure 5] may be used as templates for the *in situ* synthesis of Ag NPs. UV irradiation of the colloidal particles results in photochemical reduction of the PTA anions and thereafter, electron transfer to the Ag^+ ions from the electron-rich PTA ions and the consequent formation of Ag NPs (step 2, Figure 5). The Ag NPs are assembled predominantly on the edges of the Keggin ion framework thereby forming a 3-D super structure. The Keggin ion template may be removed by simple dissolution in an alkaline medium leaving behind reasonably intact Ag NPs super structures (step 3, Figure 5).[129]

Figure 6 shows representative SEM images recorded at different magnifications from a drop-coated film of the aqueous mixture of PTA and silver sulfate on an Si(111) substrate. Densely populated colloidal particles of the Ag^+–PTA complex are seen on the surface of the substrate. Results of Mandal et al. in this work showed the produced particles are extremely uniform in size (average size ∼2.3 mm) and exhibit well-defined morphology that appears to be predominantly rhombohedral (Figure 6).

This is much more clearly seen in the higher magnification SEM image of some of the particles (Figure 6) where the presence of spherical Ag NPs arranged along the edges in a quasi-circular fashion is observed. Thus, the high-energy edge regions

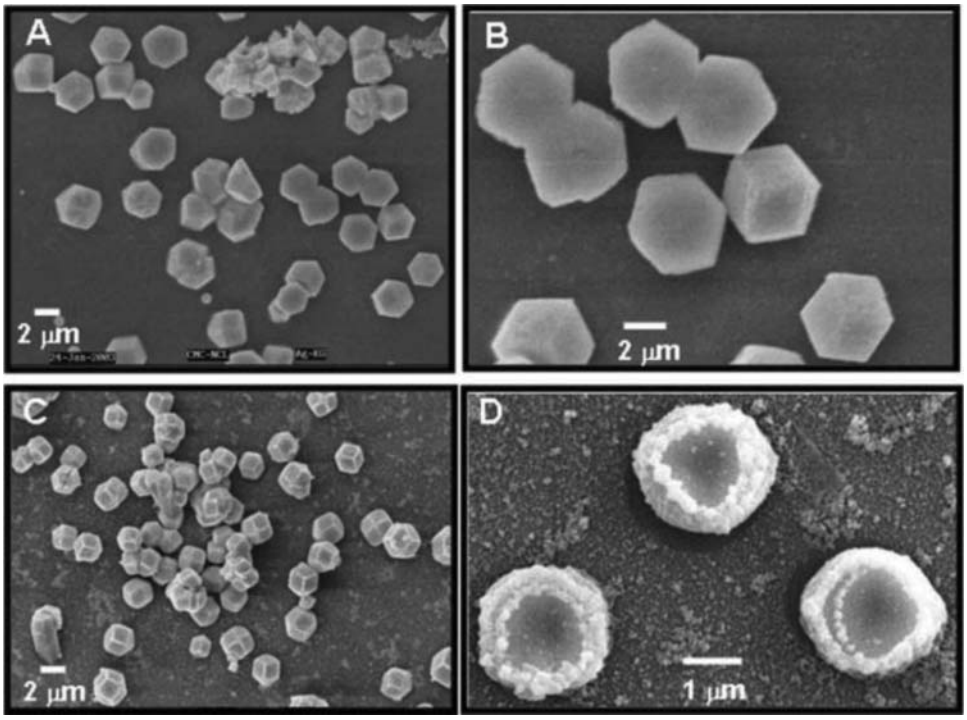

FIG. 6. (A) and (B): Low and high magnification SEM images of PTA–Ag+ ion solution before UV-irradiation, respectively. (C) and (D): Low and high magnification SEM images of PTA–Ag+ solution after UV-irradiation, respectively.[129]

of the colloidal particles play a crucial role in assembling the *in situ* formed Ag NPs. The size of Ag NPs range is from 80 to 150 nm and are thus not monodisperse.[129]

Laurent et al.[130] used Dawson-derived sandwich type POMs, $[M_4(P_2W_{15}O_{56})_2]^{16-}$, M = Co^{2+}, Ni^{2+}, and Zn^{2+} as photocatalysts and an organic substrate (propan-2-ol) as sacrificial electron donor for reduction of $Ag^I_2SO_4$ from aqueous solutions to synthesis of Ag nanoparticles. In the case of $[Co_4(P_2W_{15}O_{56})_2]^{16-}$, TEM experiments revealed that the Ag NPs obtained with a slight excess of Ag^+ are almost spherical with size in the range 20–50 nm (Figure 7). However, in a large excess of Ag^+, the obtained colloids are more oblate and assembled together to give larger aggregates.[130]

Indeed, TEM micrographs revealed that, in those concentration conditions, the Ag NPs formed using $Ni_4P_4W_{30}$ and $Zn_4P_4W_{30}$ are much smaller and more spherical compared with those obtained with $Co_4P_4W_{30}$, as their size does not exceed 30 nm. So, the central metal M of the POM seems to have an influence on the size and stability of the formed particles.[130]

In another Ag synthesis method, arginine (Arg)-tungstosilicate acid (TSA, $H_4SiW_{12}O_{40}$) solution is used for reduction of silver nitrate ($AgNO_3$) by UV irradiation, wherein the Arg-TSA complex acts as a UV-switchable reducing agent for silver ion. This method allows synthesis of spherical particles of diameter between several nanometers and several hundreds of nanometers by varying the molar ratio of silver nitrate to TSA, the pH of the reaction solution, and the reaction temperature. Arg-TSA colloidal particles act as an active organicinorganic template.[131]

In another study, one-step synthesis and stabilization of Ag nanostructures with Mo^V–Mo^{VI} mixed-valence POMs in water at room temperature has been demonstrated.[132] This method did not use a catalyst or a selective etching agent.

Ag NPs of different shape and size can be obtained using different POMs in which the POMs serve as a reductant and a stabilizer, similar to some another methods. For instance, a salt, Ag_2SO_4, and POMs, $(NH_4)_{10}[Mo^V)_4(Mo^{VI})_2O_{14}(O_3PCH_2PO_3)_2(HO_3PCH_2PO_3)_2]$-$15H_2O$, and $H_7[\beta$-$P(Mo^{VI})_4(Mo^{VI})_8$

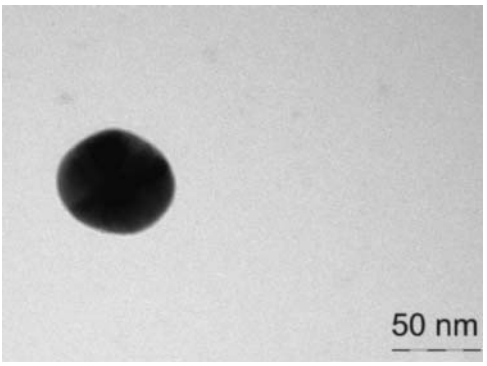

FIG. 7. TEM micrograph of Ag nanoparticles formed upon illumination of deaerated aqueous solution containing $Na_{16}[Co_4(H_2O)_2(P_2W_{15}O_{56})_2]$, propan-2-ol and Ag_2SO_4.[130]

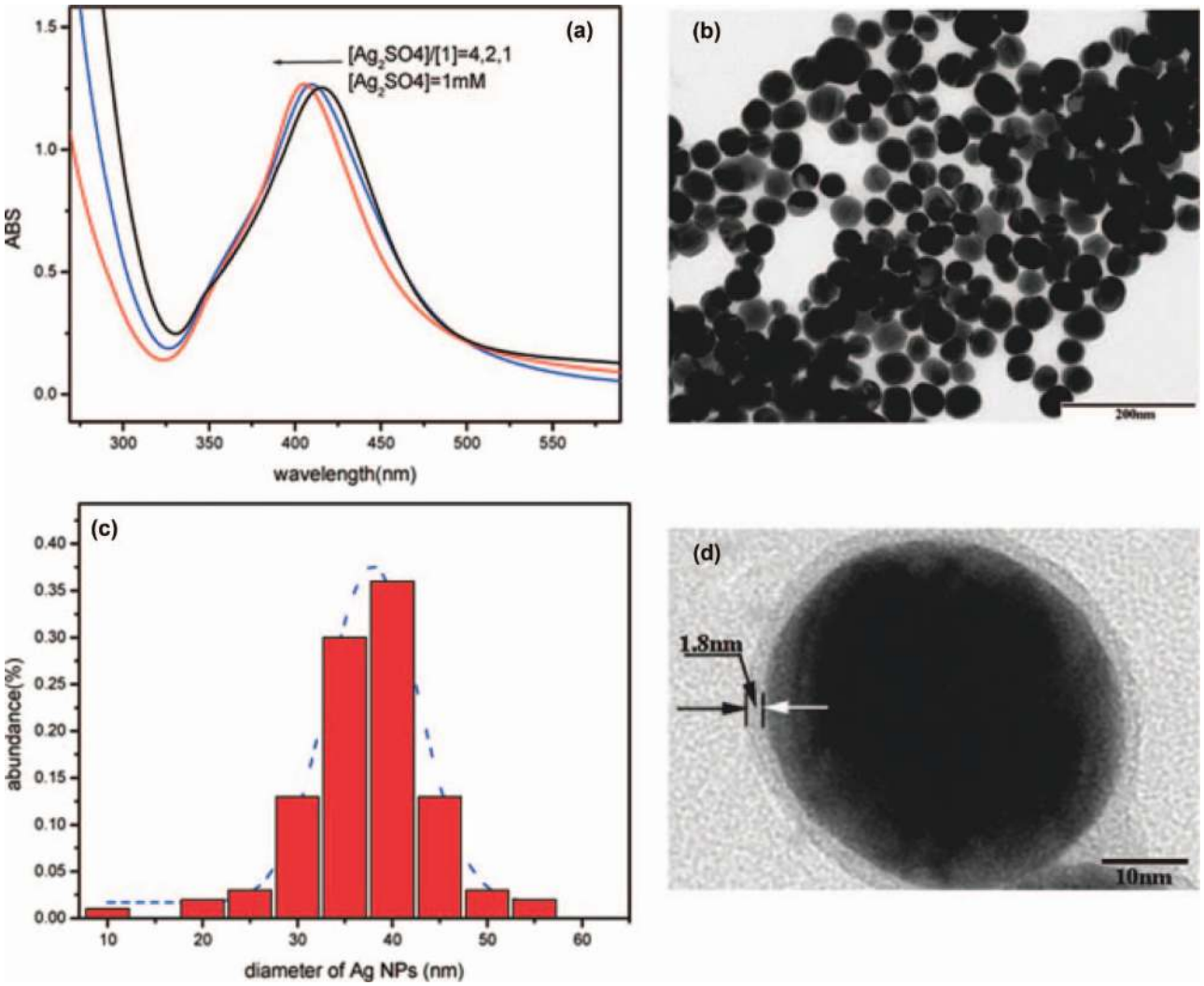

FIG. 8. (a) SPR spectra of Ag nanoparticles obtained from different molar ratios, (b) a representative TEM image of Ag nanoparticles obtained from the mixture with $\gamma = 4$, (c) size histogram of Ag nanoparticles of about 200 NPs counted from TEM image showing the distribution of Ag NPs, and (d) a magnified Ag nanoparticle[132] (color figure available online).

O_{40}], were reacted. After several minutes of mixing a characteristic SPR band at 400 nm for Ag NPs appeared and the location of the peak was not significantly affected by the initial concentration of Ag_2SO_4 (Figure 8).[132] The Ag NPs obtained were spherical and quasi-monodispersed with a diameter of 38 nm (Figure 8), the particle size distribution was quantitatively displayed in a histogram (Figure 8). The single Ag NP in Figure 5 has a Ag-POM core-shell structure with a ∼2 nm thick POM layer.

With $H_7[\beta\text{-}P(Mo^{VI})_4(Mo^{VI})_8O_{40}]$ in less than 4 h of aging, irregularly shaped Ag NPs are observed. After 4 h, short Ag nanowires were observed combined with many irregular Ag NPs. TEM analysis of a sample taken directly from the reaction mixture after 6 h of aging shows (Figure 9) that more than 95% of the image represents long nanowires, with an average diameter of ∼40 nm and a length of several tens of micrometers. The aspect ratio of the nanowires ranges from 300 to more than 1000. About 20% of nanowires show a highly twisted helical structure (Figure 9). Figure 9 gives a magnified image of a twisted helical nanowire. For better understanding of the synthesis process we can focused on Figure 10.[132]

Xu et al. investigated the preparation of Ag nanoparticles in organic-inorganic hybrid thin film by incorporation of Ag nanoparticles into dioctadecylamine (DOA)/12-molybdophosphoric acid, $[PMo_{12}O_{40}]^{3-}$, (PMo_{12}) hybrid Langmuir–Blodgett (LB) film through *in situ* reduction of PMo_{12}.[133] They employed PMo_{12} in the film, because it presents a better photochromism than most of other Keggin-type POMs and it needs much less UV irradiation time for the photochromism. This procedure is illustrated in Figure 11 (up).[133]

Their primary research confirmed the synergistic effects of DOA with PMo_{12} in the formation of Ag nanoparticles, where

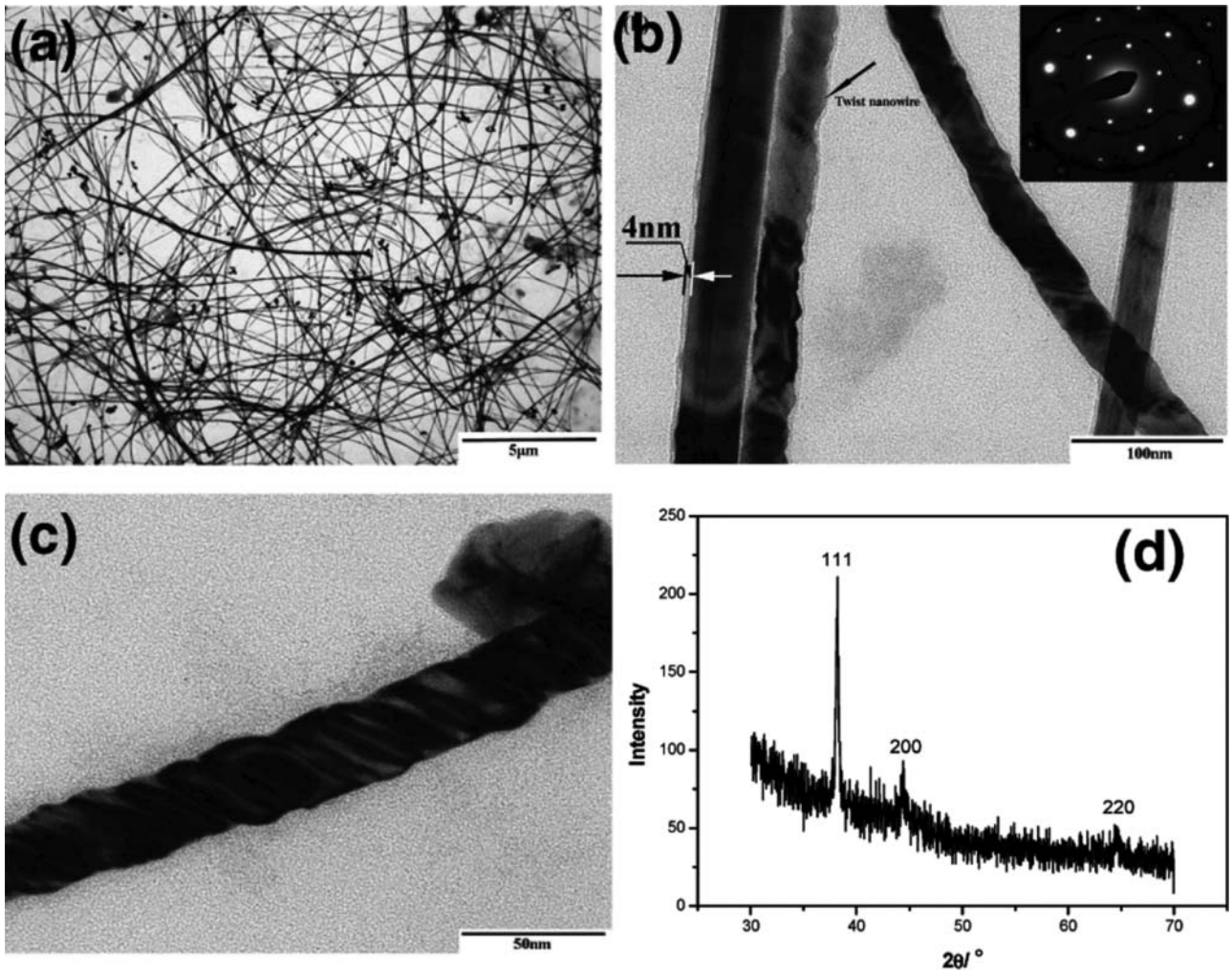

FIG. 9. (a) TEM image of as-obtained Ag nanowires directly taken from the reaction mixture, (b) magnified nanowires, (c) magnified twisted helical nanowire, and (d) XRD pattern of Ag nanowires fixed on an adhesive double-sided tape.[132]

the former supported the formation of LB film and the latter plays a role of reductant through photo-induced charge transfer complex and the enhancement for the property of PMo_{12} in the hybrid film after the formation of nanoparticles should be attributed to the interaction between the formed nanoparticles and PMo_{12}.[133]

The size distribution of produced Ag nanoparticles by Xu et al. was in a quite large range (from 2 to 25 nm) and the particles are of irregular morphology (Figure 12).[133]

GOLD NANOPARTICLES

Gold nanoparticles (Au NPs) have several applications specially as catalysts[3] and variety of methods are reported for their synthesis.

Au NPs with controllable sizes were synthesized by Troupis et al. in the presence of photochemically reduced Keggin heteropolyanions including $[SiW_{12}O_{40}]^{5-}$ and $[PW_{12}O_{40}]^{4-}$ as mild reductants and using a simple process.[25,125] They demonstrated that gold ions (Au^{III}) could form Au NPs in this condition. The TEM pattern of synthesized Au NPs indicated in Figure 13 verifies the formation of these nanoparticles with size of 13.1 ± 3.9 nm in the process.[25]

In another study, Au NPs were prepared via a simple photoreduction technique in the presence of transition metal monosubstituted Keggin heteropolyanions ($PW_{11}M$, $M = Cu^{2+}$, Ni^{2+}, Zn^{2+}, Fe^{3+}) as reducing agent, photocatalyst, and stabilizer.[134] Their interesting results indicated that the formation rate and morphology of the nanoparticles strongly depended on the kind of transition metal substituted in heteropolyacid and the preparation conditions, such as irradiation time and propan-2-ol amount. The results presented that the photoreduction rates of $PW_{11}Zn$ and $PW_{11}Fe$ were faster than those of $PW_{11}Ni$ and $PW_{11}Cu$ and the shapes of the nanoparticles synthesized in the presence of $PW_{11}Fe$ and $PW_{11}Zn$ were nearly uniform spheres, whereas the morphologies of the nanoparticles synthesized in the presence

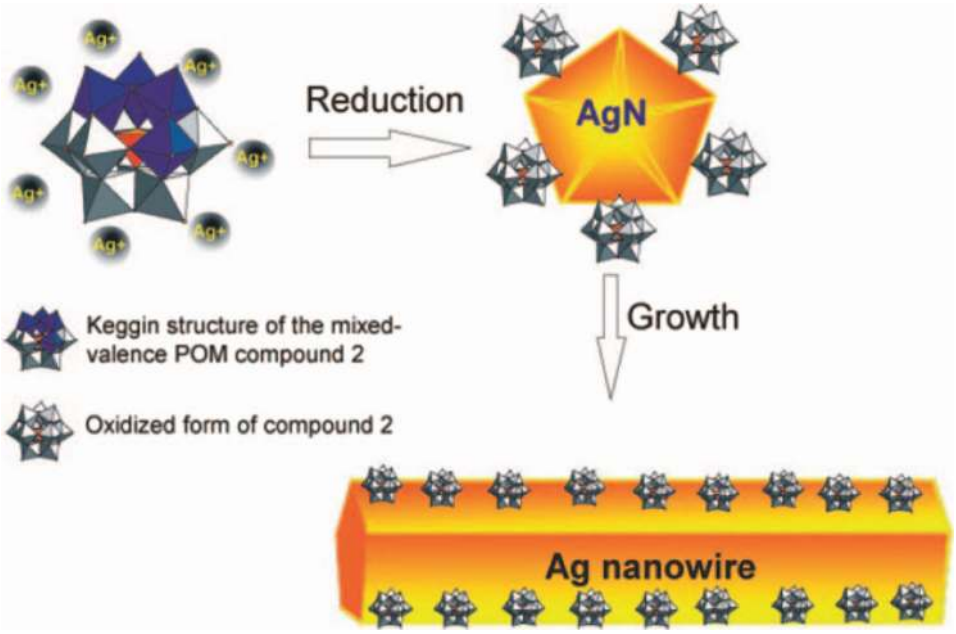

FIG. 10. Schematic picture of the process of the formation of Ag nanowires.[132]

of $PW_{11}Ni$ and $PW_{11}Cu$ were found to contain a mixture of flat triangular/hexagonal structures as well as spheres (consider Figure 14).[134]

Also, they have observed that the synthesized Au NPs in the presence of photocatalysts $PW_{11}Fe$ and $PW_{11}Zn$ are extremely stable. The lifetime of the nanoparticles obtained using photocatalyst $PW_{11}Fe$ is even longer than four months without any observable change at room temperature. In contrast, the aggregation and precipitation of the anisotropic Au NPs obtained in the presence of photocatalysts $PW_{11}Ni$ and $PW_{11}Cu$ take place easily.[134]

Previously, Systry had suggested that the formation of the gold nanotriangles is a kinetically driven process and is a result of aggregation and rearrangement of smaller-sized particles, which act as the nuclei for further growing into anisotropic, triangular structures.[135] Then the low rate of reduction of gold ions using the photocatalysts $PW_{11}Ni$ and $PW_{11}Cu$ might possibly facilitate the oriented growth of the nuclei and thus should promote the formation of anisotropic nanoparticles.[134]

As mentioned, preparation conditions have a very important role in the synthesis of nanoparticles, such as irradiation time,

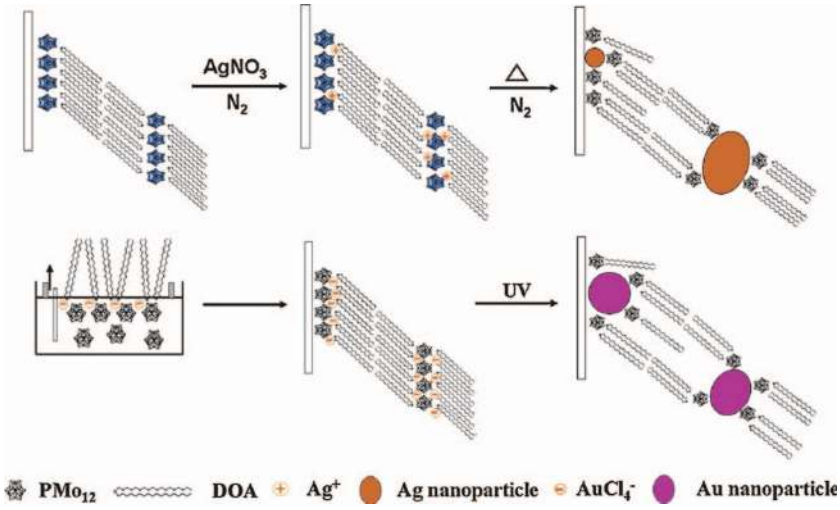

FIG. 11. Schematic drawing of silver ions penetration and formation of nanoparticles in DOA/PMo_{12} hybrid LB film (up), and preparation of $DOA\text{-}HAuCl_4/PMo_{12}$ hybrid LB film and formation of Au nanoparticles (down) (color figure available online).[133]

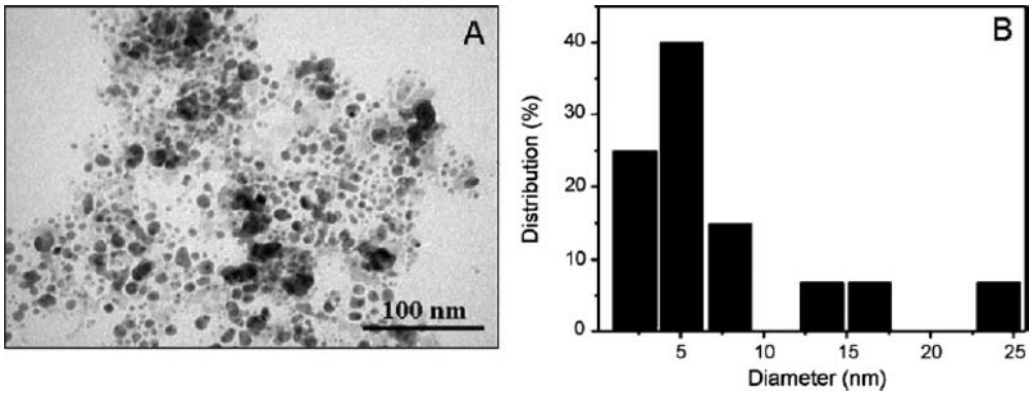

FIG. 12. (A) TEM image of silver nanoparticles by dissolving DOA/PMo_{12} LB film that encountered UV irradiation and immersion in silver ions solution in chloroform and (B) histogram of silver nanoparticles in (A).[133]

the amount of reductant, the reaction temperature, stirring rate, and coexisting ions.[135,136]

Also, increases in the irradiation time and the propan-2-ol amount could make the morphology of nanoparticles uniform and shorten the formation time of the nanoparticles. The results suggested that prolonging irradiation time will promote generation of reduced $PW_{11}Fe$, which results in a certain amount of Au NPs formation. With overextended irradiation times, the Au NPs become too large to be stable, and cause aggregation and precipitation easily. Figure 15 shows the differences in UV-Vis spectra of the Au NPs solutions synthesized in the presence of $PW_{11}M$ with two irradiation times.[134]

Shanmugam et al. used their chemical route for synthesis of Au NPs. Their method was described on Ag NPs section. As mentioned before, they described a single-step soft chemical route, in which Au NPs were embedded into the organic–inorganic composite films by dipping the reduced composite film in aqueous solution of $HAuCl_4$. The blue color of the film changed into pink indicating the formation of Au nanoparticles in the composite film.[128]

The formations of metallic Au NPs in composites were studied by TEM studies. Figure 16 shows TEM images of Au NPs embedded composite films. The formation of highly distributed Au NPs in the composite film with spherical shape can be seen with average particle size of 12 nm. In this method, the particle size can be controlled by dipping time intervals and concentration of metal ion solutions.[128]

The method of Xu et al. is described in the Ag NPs synthesis section. They used their method for synthesis of Au NPs, too. They showed that the Au ions are reduced to Au NPs in the hybrid film. But, because the volume of $AuCl_4$ ions is a negative charge and bigger than silver ions, the permeation into hybrid LB film becomes more difficult and needs much longer time.[133]

Because the Au ions can be well dispersed in LB film in a controllable way, they can obtain regular aggregated structure of the hybrid LB film under the existence of Au particles.[133]

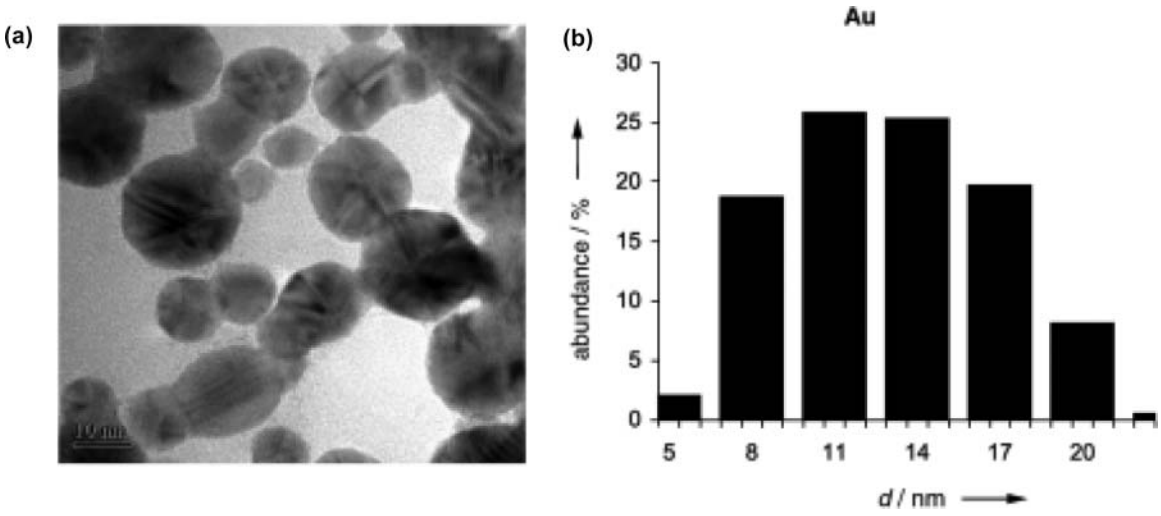

FIG. 13. (a) Transmission electron micrograph and (b) size histogram of the Au particles.[25]

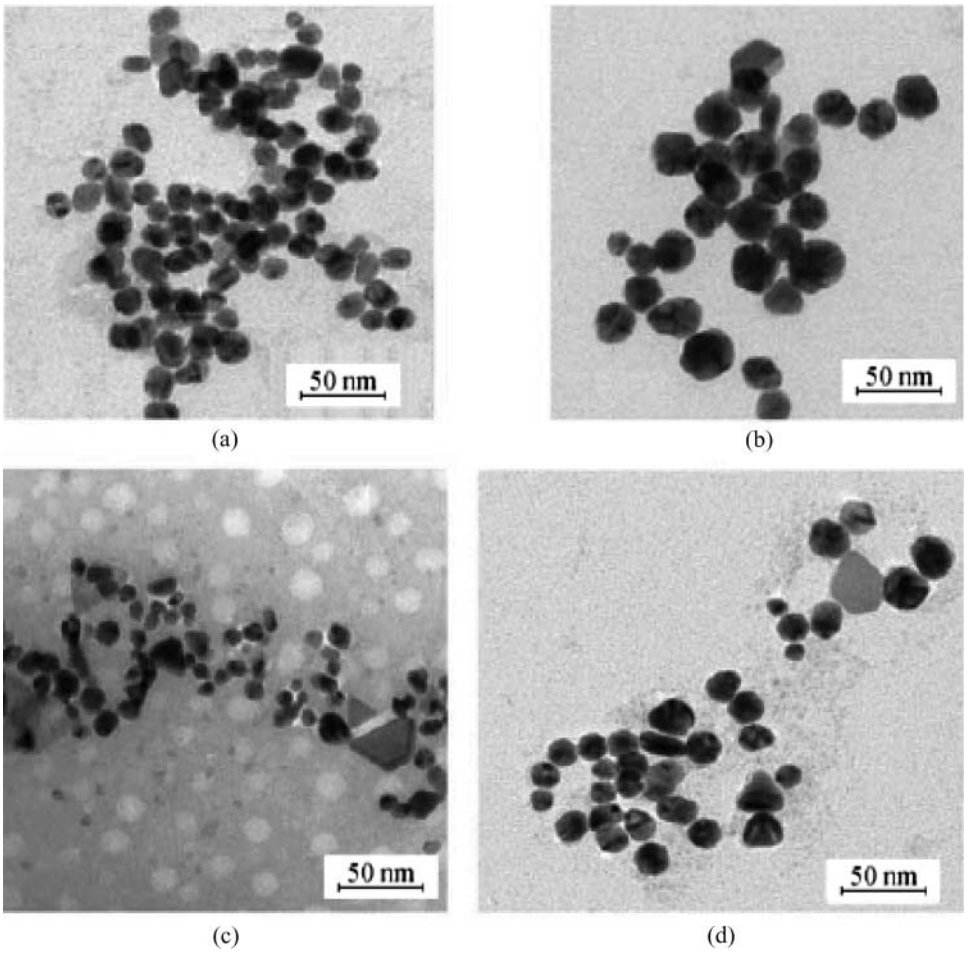

FIG. 14. TEM images of gold nanoparticles obtained in the presence of $PW_{11}M$. (a) Synthesized by $PW_{11}Fe$, irradiation time 40 min; (b) synthesized by $PW_{11}Zn$, irradiation time 40 min; (c) synthesized by $PW_{11}Ni$, irradiation time 90 min; (d) synthesized by $PW_{11}Cu$, irradiation time 90 min.[134]

Their results illustrated that the formation of Au nanoparticles in the DOA-$HAuCl_4$/PMo_{12} hybrid film is mainly derived from the reduction of PMo_{12} rather than from UV irradiation. The DOA-$HAuCl_4$/PMo_{12} single monolayer exhibits a uniformly flat morphology even at high surface pressure. The DOA-$HAuCl_4$/PMo_{12} LB film after UV irradiation can be dissolved in chloroform and cast to a copper grid for TEM observation. A TEM image of synthesized nanoparticles is shown in Figure 17. The mean diameter of the Au nanoparticles is ca. 19 ± 2 nm (Figure 17).[133]

It is interesting that the formation of Au nanoparticles can increase the speed of photochromism and the PMo_{12} can continuously convert into heteropolyblue again in the hybrid LB film after the formation of nanoparticles.[133]

Mixed-valence POMs have the potential to use in nanoparticles synthesis. In another study, one of mixed-valence POM, β-$H_3[H_4P(MoV)_4(MoVI)_8O_{40}]^{3-}$, was used as reducing agent and capping agent in water, for synthesis of various Au NPs in a one-pot, room-temperature process. Preliminary assays demonstrated that this kind of POM can easily react with chloroauric acid at room temperature to form Au nanostructures and that the reaction can be followed using its distinct color changes.[137]

The researchers investigated effect of initial concentrations of the POM and chloroauric acid on the shape and size of synthesized nanoparticles and found that by modifying the ratio of γ = [metallic salt]/[POM], the morphology of the synthesized Au nanostructure can be tuned (consider Figure 18). Figure 18 shows TEM images at two different magnifications, when $\gamma = 1$. In this ratio the NPs are spherically shaped with a diameter of around 110 nm and a scattered size distribution. A few anisotropic and irregularly shaped structures are also visible. The TEM image for $\gamma = 0.4$ and 0.1 (Figure 2) displays quasi-monodisperse nanoparticles with a diameter decreased to 70 nm, accompanied by numerous triangular and hexagonal nanoplates.[137]

Figure 19 is a schematic, which sums up the morphological possibilities during the synthesis of Au^0 nanostructures by β-$[H_4P(MoV)_4(MoVI)_8O_{40}]^{3-}$ and suggests some recyclability of the POM.[137]

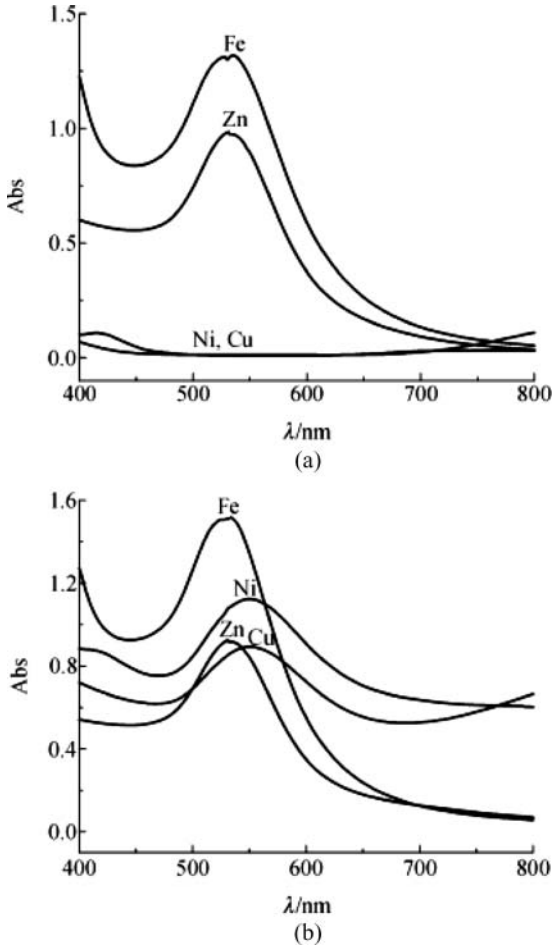

FIG. 15. UV-Vis spectra of the gold nanoparticle solutions synthesized in the presence of $PW_{11}M$. ($M = Zn^{2+}$, Fe^{3+}, Ni^{2+}, Cu^{2+}) with irradiation time 40 min (a) and irradiation time 90 min (b).[134]

Furthermore, Mandal and coworkers reported that photochemically generated $[PW_{12}O_{40}]^{4-}$-capped Au NPs enable the reduction of Ag^{+} on the surface of the Au NPs to form Au-Ag core-shell bimetallic nanoparticles under further irradiation

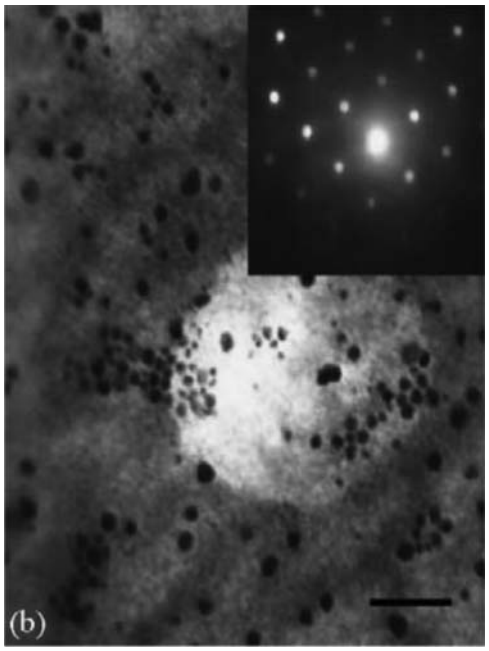

FIG. 16. Transmission electron micrographs of noble metal nanoparticles embedded composite films: Au. Insets show respective electron diffraction pattern. Scale bar 100 nm.[128]

from UV light. The characteristic of this method is that the reaction proceeds at room temperature within seconds and utilizes a mild reductant, Keggin heteropolyanion.[123]

The simple scheme of Keggin ion-mediated synthesis of Au core-Ag shell nanoparticles is shown in Figure 20. They showed representative TEM images (Figure 21) of a drop-cast film of Au core-Ag shell nanoparticles grown as described previously.[123]

As in the case of Au NPs alone, the particles are quite polydisperse, show a small increase in size (ranging from 20 to 100 nm), and are of varying morphology.[123]

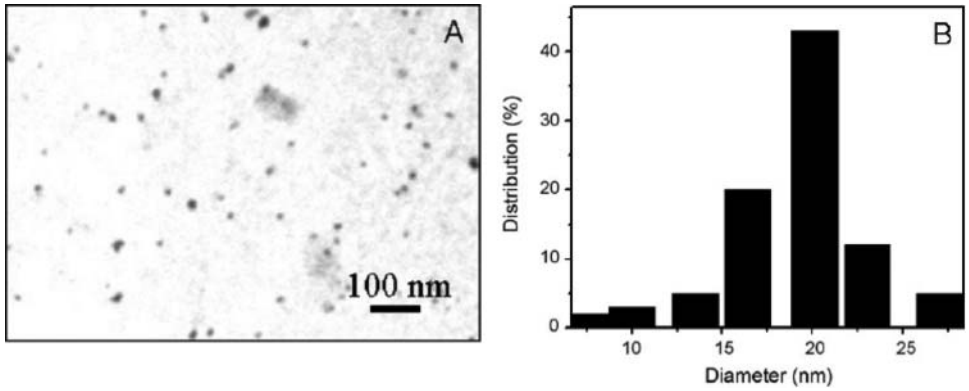

FIG. 17. (A) TEM image of Au nanoparticles after UV irradiation, prepared by dissolving DOA-$HAuCl_4$/PMo_{12} LB film in chloroform and (B) histogram of Au nanoparticles in (A).[133]

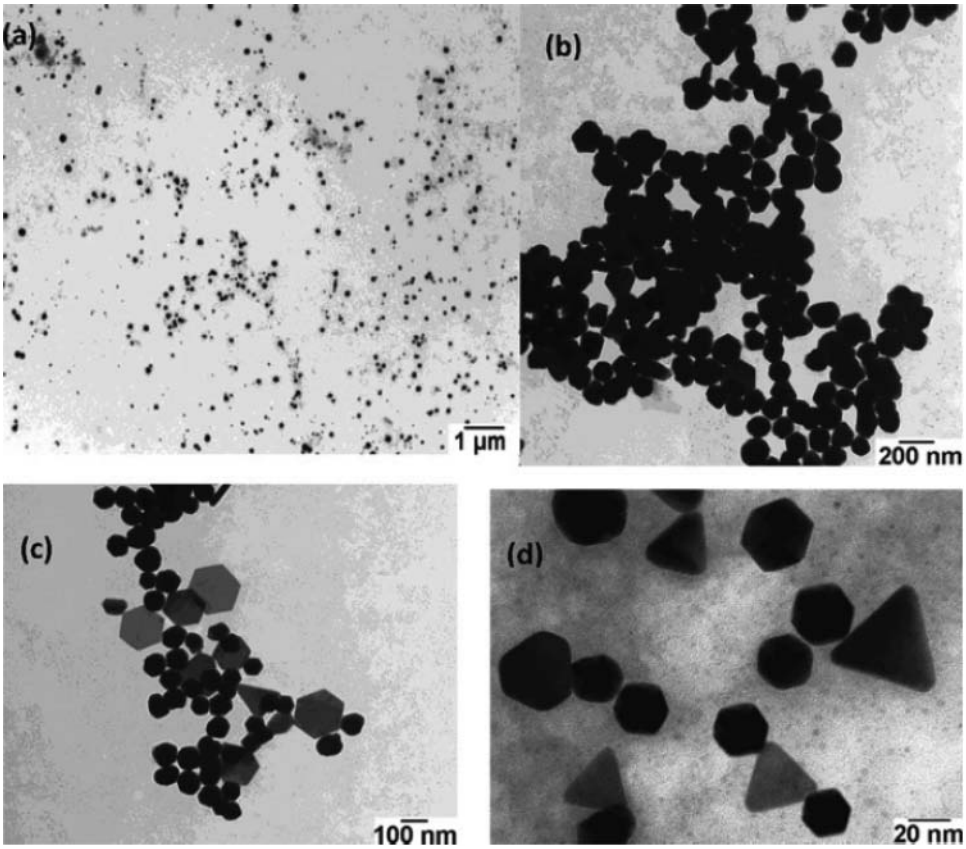

FIG. 18. TEM images of synthesized Au NPs at different molar ratios with initial concentration of POM = 1mM and (a) and (b) $\gamma = 1$, (c) $\gamma = 0.4$, and (d) $\gamma = 0.1$. Note the scale bars which show clearly the difference in size of the nanostructures prepared using various g values.[137]

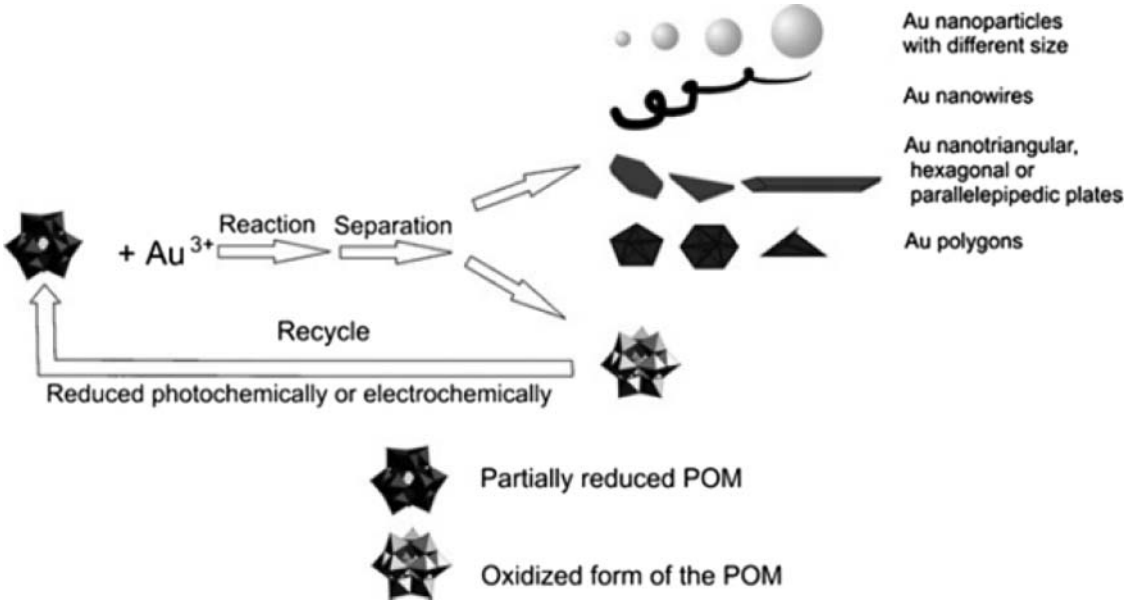

FIG. 19. Morphological possibilities during the synthesis of Au^0 nanostructures by β-$[H_4P(MoV)_4(MoVI)_8O_{40}]^{3-}$ and recyclability of the POM.[137]

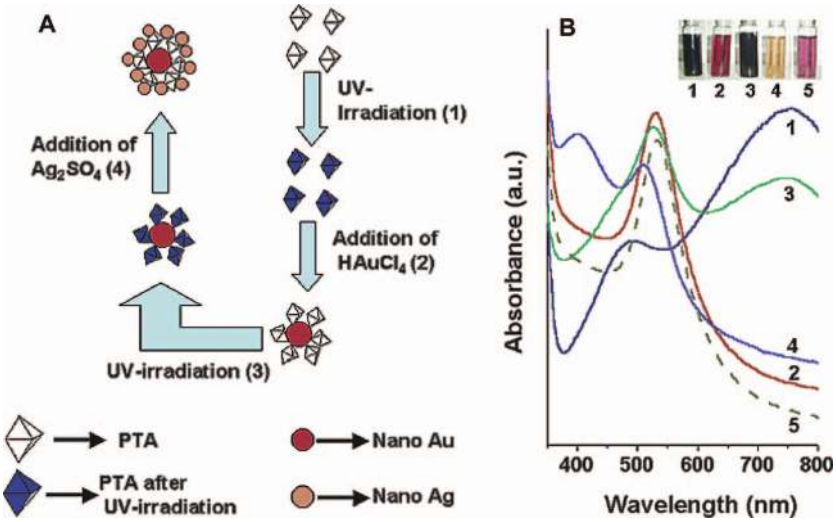

FIG. 20. (A) Scheme of the Keggin ion-mediated synthesis of Au core-Ag shell nanoparticles. For simplicity, Keggin ions are shown as octahedral particles. (B) UV-vis spectra recorded from (1) 10^{-2} M aqueous solution of PTA after UV irradiation; (2) UV-irradiated PTA solution after addition of 10^{-3} M $HAuCl_4$; (3) solution 2 after further UV irradiation; (4) solution 3 after addition of 10^{-3} M Ag_2SO_4 solution; and (5) solution 2 after addition of 10^{-3} M Ag_2SO_4. All UV-vis spectra have been adjusted for solution dilution effects. Pictures of sample bottles containing solutions 1–5 are shown in the inset[119] (color figure available online).[123]

SELENIUM NANOPARTICLES

Among all of the semiconductors, selenium is one of the most important semiconductors in view of its various applications. It has a number of attractive features desired for various applications in photonics and electronics.[138]

Equations 2–4 can be used for synthesis of selenium nanoparticles (Se NPs). Se NPs are formed upon photolysis of solutions of propan-2-ol/POM/Se(IV). Propan-2-ol serves as sacrificial reagent for the photo formation of 1-equivalent reduced blue polyoxometalate, POM(e), which further reacts with Se(IV) to produce Se NPs. POM serves both as relay for the transfer of electrons from propan-2-ol to Se(IV) and stabilizer for the nanoparticles.[124]

As discussed before, control of the size of the particles can be also achieved via rate control of Equation 4. Faster reduction of metal ion leads to smaller and more uniform nanoparticles suggesting that the rate of metal ion reduction affects strongly the initial nucleation of particles. Ionic strength and initial concentration of POM are two effective parameters in size of produced nanoparticles. As an example, changing the ionic strength from 0 to 0.025 and 0.05 M results in the formation of gradually larger nanoparticles of 40, 60, and 90 nm, respectively, and increases of the initial concentration of $(SiW_{12}O_{40})^{4-}$ from 2 to 4 and 10×10^{-3} M, resulting in the formation of gradually smaller nanoparticles, 110, 80, and 60 nm, respectively.[124]

The TEM images of the produced Se^0 nanoparticles are shown in Figure 22, while the inset in Figure 22 is the corresponding selected area electron diffraction pattern indicating the crystallinity of the Se nanoparticles. The effect of initial concentration of $(SiW_{12}O_{40})^{4-}$ is clear in this figure. The fact that smaller Se^0 nanoparticles are formed with increasing of the initial concentration of $(SiW_{12}O_{40})^{4-}$ implies that the nucleation

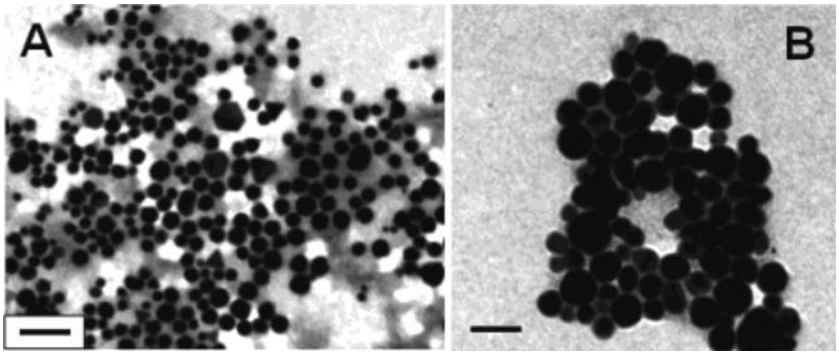

FIG. 21. (A) TEM picture of gold nanoparticles reduced by UV-irradiated PTA solution. (B) TEM picture of gold core-silver shell nanoparticles by sequential reduction of gold and silver ions by UV-irradiated PTA solution. Scale bars in A and B correspond to 100 and 50 nm, respectively.[123]

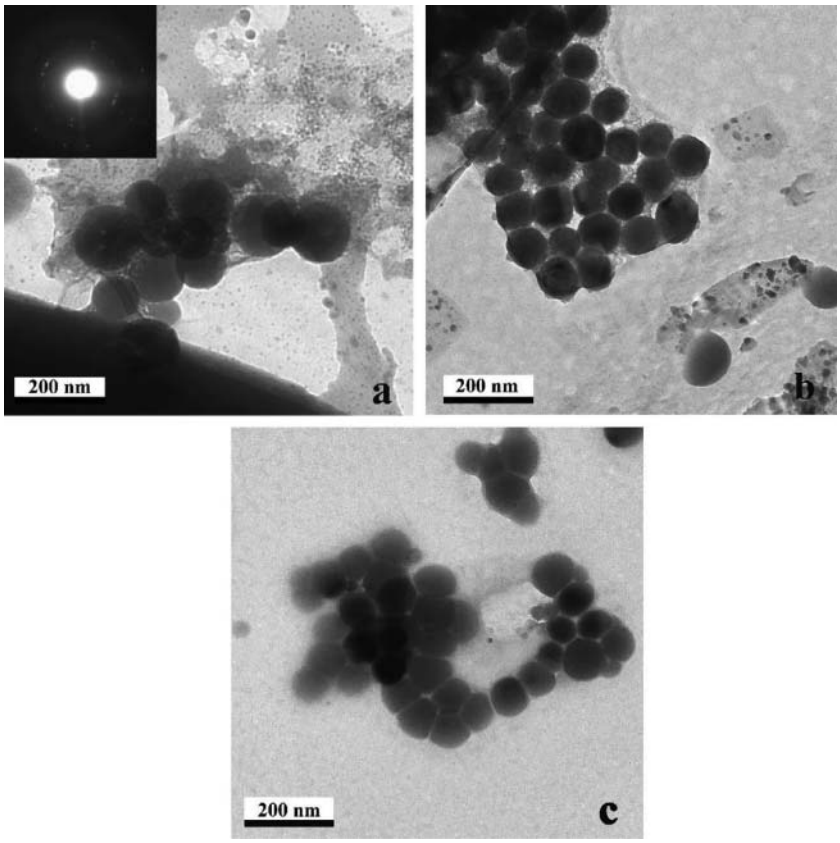

FIG. 22. TEM images of selenium nanoparticles obtained upon reduction of Se(IV) 1×10^{-3} M by various concentrations of $(SiW_{12}O_{40})^{4-}$ (a) 2×10^{-3} M, (b) 4×10^{-3} M, and (c) 10×10^{-3} M. The inset is the corresponding selected area electron diffraction pattern.[124]

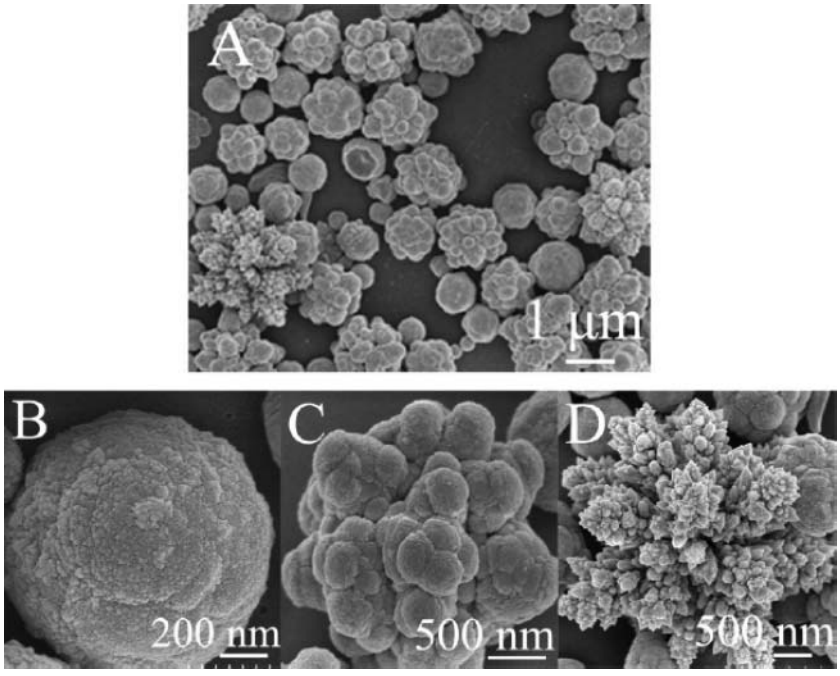

FIG. 23. SEM images of (A) CdS particles synthesized at 50°C for 48 h, and (B–D) three representative particles.[142]

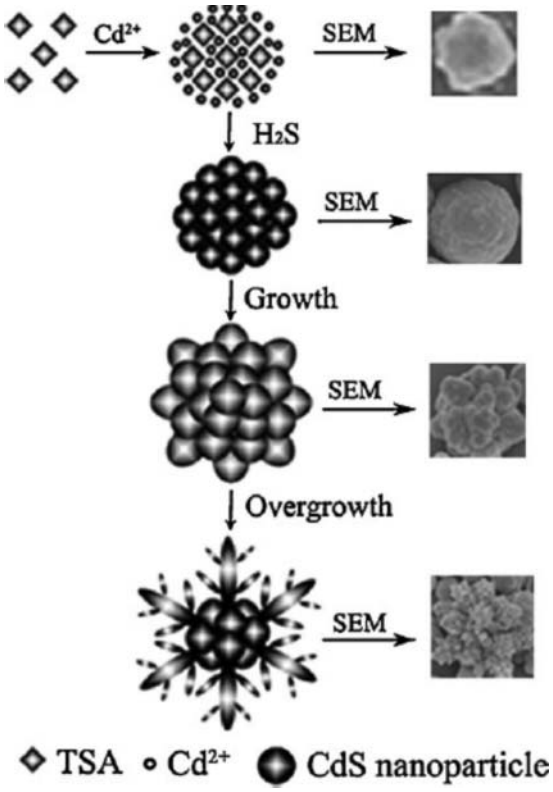

FIG. 24. The proposed evolution process of spherical CdS assembly to flower-like structure.[142]

process is enhanced more than the growth of Se^0 nanoparticles.[124]

In a study, for the synthesis of Se nanoparticles as a size-controlled method, tungstosilicate acid ($H_4SiW_{12}O_{40}$, TSA) solution that serves both as reducing reagent and stabilizer was used. In this method, selenium acid (H_2SeO_3) reduced by UV-irradiated TSA.[139]

The synthesized nanoparticles are monodisperse with sizes in diameter (∼40 nm) and have spherical colloids of t-Se (triangular-structured selenium forms. The TEM image implies these spheres are smooth. Such colloids were quite uniform and could be obtained in copious quantities. The size of nanoparticles synthesized by this method can be controlled by varying the reaction temperature.[139]

CADMIUM SULFIDE NANOPARTICLES

Cadmium sulfide (CdS) is one of the most important II-VI group semiconductors and has been used for years in solar cells and optoelectronic and electronic devices.[140,141] There are limited strategies have been used to synthesize these nanoparticles by use of POMs.

In one study, the CdS NPs have been synthesized in the combination of diffusion and hydrothermal method with type TSA as scaffold at different temperatures.[142]

In this gas diffusion–hydrothermal synthesis route, the generation of H_2S gas and the formation of the CdS products can be expressed by the following equations:[142]

$$CH_3CSNH_2 + 2H_2O \rightarrow CH_3COONH_4 + H_2S \qquad [6]$$

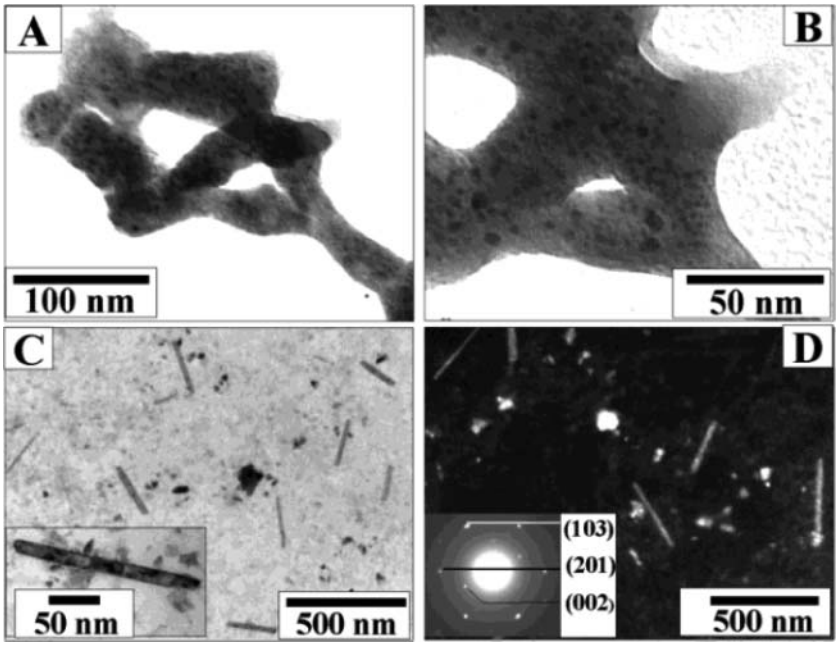

FIG. 25. (A) and (B): Low and high magnification TEM images from the Cd^{2+}-PTA solution after H_2S treatment. (C) and (D): Bright and dark field TEM images of CdS nanorods formed after the alkali treatment of the CdS-PTA solution. The inset in (C) shows an image of one of the CdS nanorods in greater detail, and the inset in (D) shows the SAED pattern of the CdS nanorods shown in (C).[143]

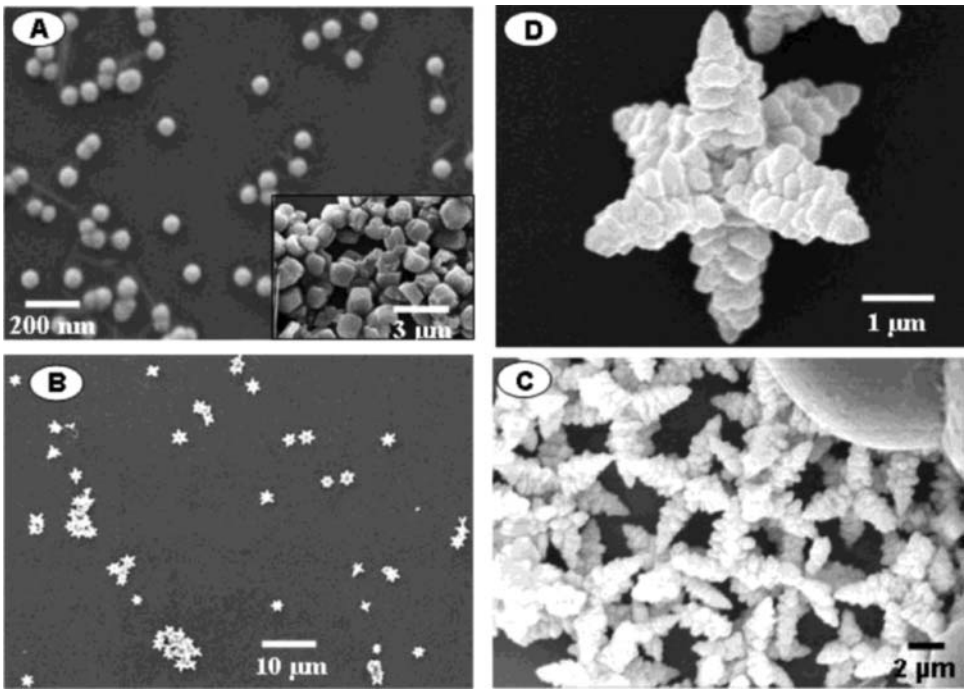

FIG. 26. SEM images recorded from (A) calcium phosphotungstate colloidal particles formed by reacting an aqueous solution of phosphotungstic acid with Ca^{2+} ions for 1 h, and (B-D) star-shaped $CaCO_3$ crystals under different stages of magnification obtained by reacting calcium phosphotungstate colloidal particles.[145]

$$Cd^{2+} + TSA \rightarrow TSA - Cd^{2+} \quad [7]$$

$$TSA - Cd^{2} + H_2S \rightarrow TSA - CdS \quad [8]$$

The precipitation of CdS is mainly controlled by the diffusion level of H_2S gas. Because Cd^{2+} can react with S^{2-} very rapidly. Mainly this parameter controls the precipitation of CdS. When the diffusion rate is slow, diffusion controlled growth is dominant, which leads to continual structure rearrangement and extension growth.[142]

In this study, it was found that the evolution of CdS microsphere to flowerlike structure can be modulated by tuning the diffusion rate of H_2S gas, which is dominated by the reaction temperature. Slow diffusion rate of H_2S gas leads to a flowerlike morphology (Figure 23) and fast diffusion rate leans to a spherical morphology. A possible mechanism for the evolution is proposed by Zhang et al., that slow diffusion rate of H_2S gas favors the diffusion-controlled growth, and fast diffusion rate promotes a reaction controlled growth.[142]

Also, they proposed a clear growth mechanism like Figure 24. At the first stage, spherical CdS particles obtained from

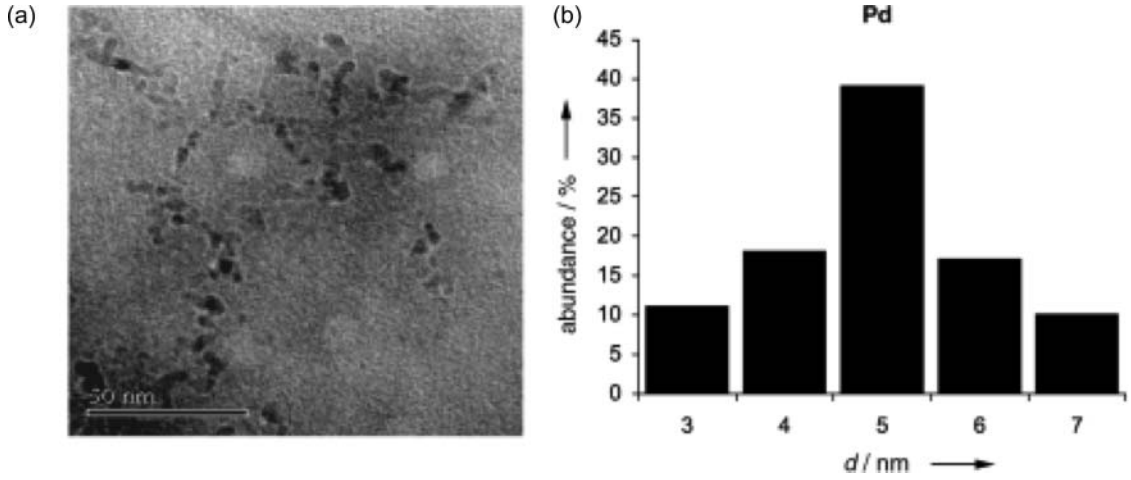

FIG. 27. (a) Transmission electron micrograph and (b) size histogram of the Pd particles.[25]

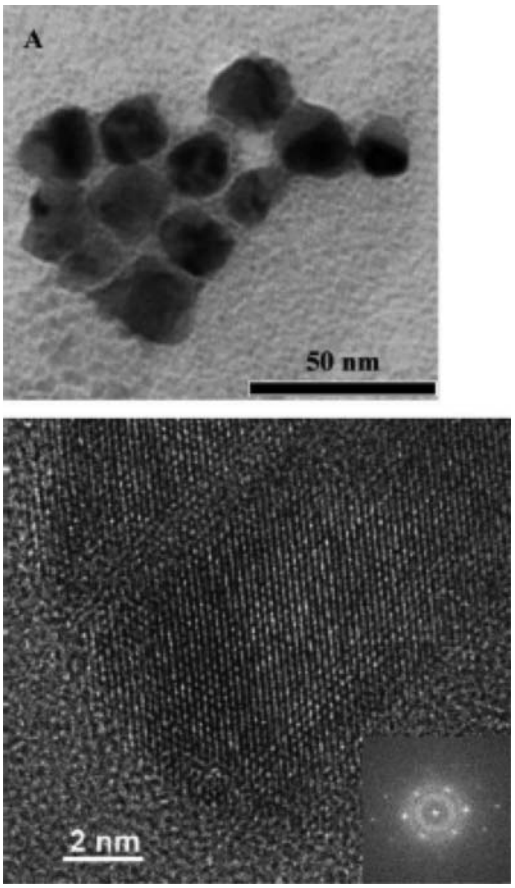

FIG. 28. (A) Typical TEM image of palladium nanocrystals synthesized at the K_2PdCl_4/HPV^{IV} molar ratio of 0.5. (B) High-resolution TEM image and electron diffraction pattern of Pd nanoparticles showing the crystal lattice of Pd atoms.[149]

spherical TSA-Cd^{2+} precursor, which is played a key role on the *in situ* formation of spherical CdS assemblies. After that, H_2S atmosphere promotes a diffusion-controlled growth process, in which the petals appeared from the primal multiplayer surface structure and then flowerlike structure formed.[142]

Likewise, reaction of aqueous cadmium cations with phosphotungstate Keggin anions (PTA) leads to the growth of highly dense and crystalline cadmium phosphotungstate colloidal particles with needlelike morphology of submicron dimensions. Further treatment of these particles with H_2S gas leads to the *in situ* growth of CdS nanoparticles of 5–6 nm sizes without disruption to the host Keggin ion colloidal particle morphology. Alkali treatment results in dissolution of the PTA template, leaving behind fused CdS nanoparticles in the form of nanorods (see Figure 25).[143]

CALCIUM CARBONATE NANOPARTICLES

Calcium carbonate nanocrystal has wide applications in rubber, plastic, printing ink, oil point, toothpaste, cosmetics, and food industries because of its low cost and excellent physical and chemical properties. Many chemical techniques were used to prepare of them.[144] To the best of our knowledge, there are not many reports on synthesis of calcium carbonate nanocrystals using POMs.

Rautaray et al. have been shown that Keggin anions complexed with Ca^{2+} can play role of template for growth of $CaCO_3$ crystals. Reaction of an aqueous solution of phosphotungstic acid with Ca^{2+} ions leads to the formation of highly uniform, stable colloidal particles of calcium phosphotungstate, which may then be reacted with CO_2 results in the growth of star-shaped $CaCO_3$ crystals with uniform size in solution.[145]

An SEM image recorded from a drop-cast film of the solution obtained by reaction of aqueous $CaCl_2$ and $H_3PW_{12}O_{40}$ on an Si (111) substrate is shown in Figure 26. Colloidal particles have spherical morphology and average particle size of 57 ± 8 nm. Figure 26 shows SEM images at different magnifications recorded after the formation of $CaCO_3$ crystals by bubbling CO_2 into the calcium phosphotungstate colloidal particle solution.[145]

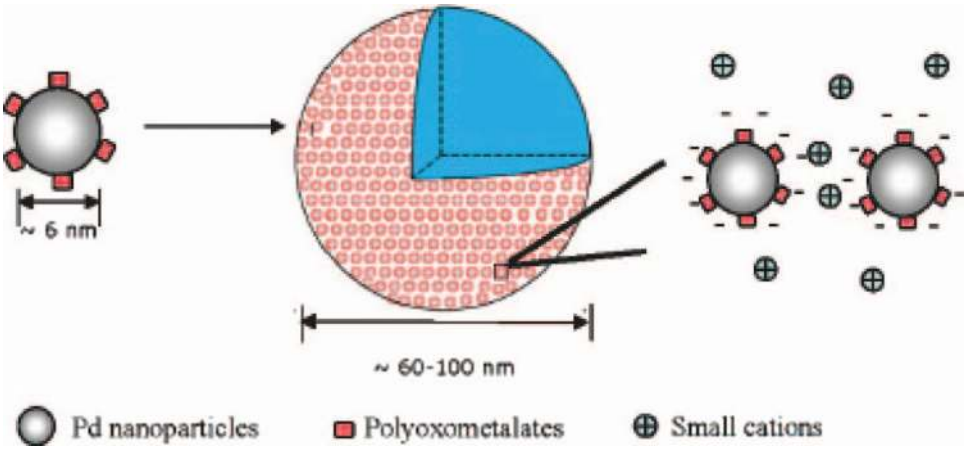

FIG. 29. The 3-nm-radius Pd nanoparticles with a layer of POM HPV^{IV} or HPV^{V} on the surface self-organize into large, hollow 60–100 nm aggregates. Small counter-ion cations might be incorporated into the large hollow structures[149] (color figure available online).

PALLADIUM NANOPARTICLES

Palladium nanoparticles (Pd NPs) have been reported to be very active and selective in a wide range of reactions including hydrogenations, C–C coupling and oxidations. The preparation of small, stable Pd NPs still remains a challenging task.[146]

For efficient synthesis and stabilization of Pd NPs, reduced POMs were used both as reducing and capping agents at room temperature in water.[132] They succeeded to prepare Pd nanoparticles with size of 5.0 ± 1.1 nm (Figure 27).[25]

POM catalysts are more efficient in reductive recovery of palladium. Using the POM anions as photocatalysts and propan-2-ol as sacrificial electron donor, Pd^{2+} can be reduced and recovered in metallic form.[147]

Troupis et al. indicated that palladium ions (Pd^{2+}) could form Pd nanoparticles in the presence of photochemically reduced Keggin heteropolyanions $[SiW_{12}O_{40}]^{5-}$ and $[PW_{12}O_{40}]^{4-}$ as mild reductants.[25]

In a method, it has been demonstrated that photochemically reduced POMs of the Keggin structure $[(PW_{12}O_{40})]^{3-}$ when exposed to aqueous $Pd(NO_3)_2$ resulted in the formation of Pd NPs. The results have been shown a multifunctional catalyst consisting of the Pd core capped with the Keggin ion shell that showed excellent activity in acylation reactions.[125]

Dolbecq et al. reported an illustration to the POM-based mild synthesis of metallic nanoparticles like Pt and Pd in water at room temperature.[148] In their experiments, electrochemically deposited films have been obtained from the reduction of the hexanuclear POM, which are very efficient both as reductants of Pt and Pd metallic salts and as capping agents for the resulting Pt^0 and Pd^0 nanoparticles. They used isolated different cyclic anions with the general formula $[(MoV_2O_4)(O_3PCH_2PO_3)]_n$, $(n = 3, 4, 10)$, that incorporate small organic or inorganic guests as a template and counter ion in the structure of the cyclic anions. They found that the size of the obtained nanoparticles depends both on the nature of the POM and on the [metallic salt]/[POM] ratio.[148]

Some authors reported a method of making Pd^0 nanoparticles by reducing K_2PdCl_4 via Dawson-type vanadium-substituted POM, $K_9[H_4PV^{IV}W_{17}O_{62}]$ (HPV^{IV}), in water at room temperature.[24] HPV^{IV} acted simultaneously as both the reducing agent (in which it would be oxidized to HPV^{V}) and the stabilizer.[24]

The neutral Pd nanoparticle can absorb a layer of HPV (either HPV^{IV} or HPV^{V}) on its surface, making the overall nanoparticle negatively charged with a relatively hydrophilic surface. The solution behavior of such POM-coated Pd nanoparticles is still completely unknown. The POM-coated Pd0 nanoparticles are very stable in solution, showing similarities to POM macroanions.[149]

The shape and size of formation nanoparticles is dependent on the starting molar ratio of K_2PdCl_4 to HPV^{IV} in solution. Zhang et al. showed that when this ratio is less than 0.6, ~20 nm-radius Pd^0 colloidal nanocrystals are formed (see Figure 28) and when it is greater than 0.6, HPV-capped (and therefore negatively charged) 3-nm-radius Pd^0 nanoparticles are formed, which can further self-assemble into stable, hollow, spherical, 30–50-nm-radius supramolecular structures in solution without precipitation (consider Figure 29). A higher molar ratio of K_2PdCl_4 to HPV^{IV} corresponds to a slower reduction rate and a faster growing process. Hence, the formation of larger nanocrystals can be expected.[149]

REFERENCES

1. Iskandar, F. Nanoparticle processing for optical applications: a review. *Adv. Powder Technol.* **2009**, *20*, 283–292.
2. Tsoukalas, D.; Dimitrakis, P.; Kolliopoulou, S.; Normand, P. Recent advances in nanoparticle memories. *Mater. Sci. Eng., B* **2005**, *124–125*, 93–101.
3. Hutchings, G.J. Catalysis by gold. *Catal. Today* **2005**, *100*, 55–61.
4. Molina, L.M.; Hammer, B. Some recent theoretical advances in the understanding of the catalytic activity of Au. *Appl. Catal., A* **2005**, *291*, 21–31.
5. Cai, X.; Conley, S.; Naash, M. Nanoparticle applications in ocular gene therapy. *Vision Research* **2008**, *48*, 319–324.
6. Yuan, Q.; Venkatasubramanian, R.; Hein, S.; Misra, R.D.K. A stimulus-responsive magnetic nanoparticle drug carrier: Magnetite encapsulated by chitosan-grafted-copolymer. *Acta Biomaterialia* **2008**, *4*, 1024–1037.
7. Tolaymat, T.M.; Badawy, A.M.E.; Genaidy, A.; Scheckel, K.G.; Luxton, T.P.; Suidan, M. An evidence-based environmental perspective of manufactured silver nanoparticle in synthesis and applications: a systematic review and critical appraisal of peer-reviewed scientific papers. *Sci. Total Environ.* **2010**, *408*, 999–1006.
8. Ionescu, R.; Hoel, A.; Granqvist, C.G.; Llobet, E.; Heszler, P. Low-level detection of ethanol and H_2S with temperature-modulated WO_3 nanoparticle gas sensors. *Sens. Actuators, B* **2005**, *104*, 132–139.
9. Juuti, M.; Koivunen, K.; Silvennoinen, M.; Paulapuro, H.; Peiponen, K.-E. Light scattering study from nanoparticle-coated pigments of paper. *Colloids Surf., A* **2009**, *352*, 94–98.
10. Dimitrijevic, N.M.; Kamat, P.V. Photoelectrochemistry in particulate systems. 8. Photochemistry of colloidal selenium. *Langmuir* **1988**, *4*, 782–784.
11. Frattini, A.; Pellegri, N.; Nicastro, D.; de Sanctis, O. Effect of amine groups in the synthesis of Ag nanoparticles using aminosilanes. *Mater. Chem. Phys.* **2005**, *94*, 148–152.
12. Zhang, J.; Wang, H.; Bao, Y.; Zhang, L. Nano red elemental selenium has no size effect in the induction of seleno-enzymes in both cultured cells and mice. *Life Sciences* **2004**, *75*, 237–244.
13. Kim, F.; Song, J.H.; Yang, P. Photochemical synthesis of gold nanorods. *J. Am. Chem. Soc.* **2002**, *124*, 14316–14317.
14. Niidome, Y.; Nishioka, K.; Kawasaki, H.; Yamada, S. Rapid synthesis of gold nanorods by the combination of chemical reduction and photoirradiation processes; morphological changes depending on the growing processes. *Chem. Commun.* **2003**, 2376–2377.
15. Zhu, Y.; Qian, Y.; Huang, H.; Zhang, M. Preparation of nanometer-size selenium powders of uniform particle size by [gamma]-irradiation. *Mater. Lett.* **1996**, *28*, 119–122.
16. Yu, Y.-Y.; Chang, S.-S.; Lee, C.-L.; Wang, C.R.C. Gold nanorods: electrochemical synthesis and optical properties. *J. Phys. Chem. B* **1997**, *101*, 6661–6664.
17. Chen, W.; Cai, W.; Zhang, L.; Wang, G. Sonochemical processes and formation of gold nanoparticles within pores of mesoporous silica. *Colloid Interface Sci.* **2001**, *238*, 291–295.
18. Wang, X.; Zheng, X.; Lu, J.; Xie, Y. Reduction of selenious acid induced by ultrasonic irradiation–formation of Se nanorods. *Ultrason. Sonochem.* **2004**, *11*, 307–310.
19. Anastas, P.T.; Warner, J.C. *Green Chemistry, Theory and Practice*; Oxford University Press: New York, **1998**.

20. Clark, J.H. Green chemistry: challenges and opportunities. *Green Chemistry* **1999**, *1*, 1.
21. Sharma, V.K.; Yngard, R.A.; Lin, Y. Silver nanoparticles: green synthesis and their antimicrobial activities. *Adv. Colloid. Interface. Sci.* **2009**, *145*, 83–96.
22. Papaconstantinou, E. Photochemistry of polyoxometallates of molybdenum and tungsten and/or vanadium. *Chem. Soc. Rev.* **1989**, *18*, 1–31.
23. Wang, E.B.; Hu, C.W.; Xu, L. *Introduction to Polyacid Chemistry*; Chemical Industry Press: Beijing, **1998**.
24. Keita, B.; Mbomekalle, I.-M.; Nadjo, L.; Haut, C. Tuning the formal potentials of new V^{IV}-substituted Dawson-type polyoxometalates for facile synthesis of metal nanoparticles. *Electrochem. Commun.* **2004**, *6*, 978–983.
25. Troupis, A.; Hiskia, A.; Papaconstantinou, E. Synthesis of metal nanoparticles by using polyoxometalates as photocatalysts and stabilizers. *Angew. Chem. Int. Ed.* **2002**, *41*, 1911–1913.
26. Heravi, M.M.; Sadjadi, S.; Sadjadi, S.; Oskooie, H.A.; Bamoharram, F.F. A convenient synthesis of bis(indolyl)alkanes under ultra sonic irradiation using silica-supported Preyssler nano particles. *Ultrason. Sonochem.* **2009**, *16*, 718–720.
27. Heravi, M.M.; Bakhtiari, K.; Fatehi, A.; Bamoharram, F.F. A convenient synthesis of bis(indolyl)methanes catalyzed by diphosphooctadecatungstic acid. *Catal. Comm.* **2008**, *9*, 289–292.
28. Heravi, M.M.; Sadjadi, S.; Sadjadi, S.; Oskooie, H.A.; Shoar, R.H.; Bamoharram, F.F. Silica-supported Preyssler nanoparticles as new catalysts in the synthesis of 4(3H)-quinazolinones. *S. Afr. J. Chem.* **2009**, *62*, 1–4.
29. Heravi, M.M.; Rasmi, V.; Bamoharram, F.F.; Sadjadi, S.; Fotouhi, L.; Sadjadi, S.; Bakavoli, M. Synthesis of isobenzofuran-1(3H)-ones with the aid of silica-supported Preyssler nanoparticles. *Synth. Commun.* **2009**, *39*, 4109–4116.
30. Heravi, M.M.; Sadjadi, S.; Sadjadi, S.; Oskooie, H.A.; Bamoharram, F.F. Rapid and efficient synthesis of 4(3H)-quinazolinones under ultra sonic irradiation using silica-supported Preyssler nano particles. *Ultrason. Sonochem.* **2009**, *16*, 708–710.
31. Bamoharram, F.F.; Heravi, M.M.; Heravi, H.M.; Dehghan, M. Photocatalytic oxidation of benzyl alcohols in the presence of $H_{14}[NaP_5W_{30}O_{110}]$ as a green and reusable catalyst. *Synth. React. Inorg. Met.-Org. Chem.* **2009**, *39*, 394–399.
32. Bamoharram, F.F.; Heravi, M.M.; Mehdizadeh, S. Preyssler anion as a green and eco-friendly catalyst for photocatalytic oxidation of aromatic aldehydes. *Synth. React. Inorg. Met.-Org. Nano-Met. Chem.* **2009**, *39*, 746–750.
33. Heravi, M.M.; Behbahani, F.K.; Bamoharram, F.F. Acetylation of alcohols, phenols and salicylic acid by heteropoly acids in acetic anhydride: a green and eco-friendly protocol for synthesis of acetyl salicylic acid (aspirin). *Arkivoc* **2007**, 123–131.
34. Gharib, A.; Scheeren, J.W.; Bamoharram, F.F.; Roshani, M.; Jahangir, M. Acetylation of p-Aminophenol by Preyssler's anion $[NaP_5W_{30}O_{110}]^{(14-)}$, $[NaP_5W_{29}MoO_{110}]^{(14-)}$ with green condition at room temperature. *Pol. J. Chem. Tech.* **2009**, *11*, 31–35.
35. Heravi, M.M.; Beheshtia, Y.S.; Khorshidi, M.; Baghernejad, B.; Bamoharram, F.F. Application of heteropolyacids as heterogeneous and recyclable catalysts for one-pot synthesis of 3-cyanopyridine derivatives. *Chin. J. Chem.* **2009**, *27*, 569–572.
36. Heravi, M.M.; Bakhtiari, K.; Zadsirjan, V.; Bamoharram, F.F.; Heravi, O.M. Aqua mediated synthesis of substituted 2-amino-4H-chromenes catalyzed by green and reusable Preyssler heteropolyacid. *Bioorg. Med. Chem. Lett.* **2007**, *17*, 4262–4265.
37. Heravi, M.M.; Motamedi, R.; Bamoharram, F.F.; Seify, N. A catalytic method for synthesis of 6-aryl-1H-pyrazolo[3,4-d]pyrimidin-4[5H]-ones by heteropolyacids: $H_{14}[NaP_5W_{29}MoO_{110}]$ and $H_3PMo_{12}O_{40}$. *Catal. Commun.* **2007**, *8*, 1467–1471.
38. Bamoharram, F.F.; Heravi, M.M.; Roshani, M.; Gharib, A.; Jahangir, M. A catalytic method for synthesis of γ-butyrolactone, ε-caprolactone and 2-cumaranone in the presence of Preyssler's anion, $[NaP_5W_{30}O_{110}]^{14-}$, as a green and reusable catalyst. *J. Mol. Catal. A: Chem.* **2006**, *252*, 90–95.
39. Bamoharram, F.F.; Heravi, M.M.; Roshani, M.; Gharib, A.; Jahangir, M. Catalytic method for synthesis of aspirin by a green, efficient and recyclable solid acid catalyst (Preyssler's anion) at room temperature. *J. Chin. Chem. Soc.* **2007**, *54*, 1017–1020.
40. Heravi, M.M.; Derikvand, F.; Bamoharram, F.F. A catalytic method for synthesis of Biginelli-type 3,4-dihydropyrimidin-2 (1H)-one using 12-tungstophosphoric acid. *J. Mol. Catal. A: Chem.* **2005**, *242*, 173–175.
41. Bamoharram, F.F.; Heravi, M.M.; Roshani, M.; Abrishami, F. Catalytic N-oxidation of picolinic acid in the presence of heteropolyacids including Mo and W. *J. Mol. Catal. A: Chem.* **2007**, *267*, 241–244.
42. Heravi, M.M.; Ranjbar, L.; Derikvand, F.; Oskooie, H.A.; Bamoharram, F.F. Catalytic oxidative cleavage of CN bond in the presence of mixed-addenda vanadomolybdophosphate, $H_6PMo_9V_3O_{40}$ as a green and reusable catalyst. *J. Mol. Catal. A: Chem.* **2007**, *265*, 186–188.
43. Bamoharram, F.F.; Heravi, M.M.; Roshani, M.; Akbarpour, M. Catalytic performance of Preyssler heteropolyacid as a green and recyclable catalyst in oxidation of primary aromatic amines. *J. Mol. Catal. A: Chem.* **2006**, *255*, 193–198.
44. Hekmatshoar, R.; Heravi, M.M.; Sadjadi, S.; Oskooie, H.A.; Bamoharram, F.F. Catalytic performance of Preyssler heteropolyacid,$[NaP_5W_{30}O_{110}]^{14-}$ in liquid phase alkylation of phenol with 1-octene. *Catal. Commun.* **2008**, *9*, 837–841.
45. Bamoharram, F.F.; Roshani, M.; Heravi, M.M.; Safaie, S. The catalytic performance of Preyssler's anion, $[NaP_5W_{30}O_{110}]^{(14-)}$, in the oxidation of benzyl alcohols. *Phosphorus, Sulfur Silicon Relat. Elem.* **2006**, *181*, 2833–2841.
46. Heravi, M.M.; Motamedi, R.; Seifi, N.; Bamoharram, F.F. Catalytic synthesis of 6-aryl-1H-pyrazolo[3,4-d]pyrimidin-4[5H]-ones by heteropolyacid: $H_{14}[NaP_5W_{30}O_{110}]$ and $H_3PW_{12}O_{40}$. *J. Mol. Catal. A: Chem.* **2006**, *249*, 1–3.
47. Heravi, M.M.; Sadjadi, S.; Hekmatshoar, R.; Oskooie, H.A.; Bamoharram, F.F. Deamination of some N-amino nitrogen heterocycles using Preyssler's anion. *Monatshefte Fur Chemie* **2008**, *139*, 107–110.
48. Heravi, M.M.; Sadjadi, S.; Hekmatshoar, R.; Oskooie, H.A.; Bamoharram, F.F. Dehydration of oximes to nitriles catalyzed by a green heteropolyacid catalyst: Preyssler's anion, $[NaP_5W_{30}O_{110}]^{(14-)}$. *Chin. J. Chem.* **2009**, *27*, 607–609.
49. Sadjadi, S.; Heravi, M.M.; Poormohammad, N.; Oskooie, H.A.; Beheshtiha, Y.S.; Bamoharram, F.F. Direct oxidative conversion of benzoyl chlorides to 2-imidazoles using heteropolyacids. *Synth. Commun.* **2009**, *39*, 3119–3125.
50. Heravi, M.M.; Sadjadi, S.; Oskooie, H.A.; Shoar, R.H.; Bamoharram, F.F. A direct oxidative route for the synthesis of pyrimidines using heteropolyacids. *Tetrahedron Lett.* **2009**, *50*, 662–666.
51. Heravi, M.M.; Derikvand, F.; Bamoharram, F.F. Dodecatungstophosphoric acid ($H_3PW_{12}O_{40}$): A novel and efficient recyclable catalyst for synthesis of 1,1-diacetates from aromatic aldehydes in solvent-free system and their deprotection. *Synth. Commun.* **2006**, *36*, 3109–3115.
52. Heravi, M.M.; Rajabzadeh, G.; Bamoharram, F.F.; Seifi, N. An eco-friendly catalytic route for synthesis of 4-amino-pyrazolo[3,4-d]pyrimidine derivatives by Keggin heteropolyacids under classical heating and microwave irradiation. *J. Mol. Catal. A: Chem.* **2006**, *256*, 238–241.
53. Bamoharram, F.F.; Heravi, M.M.; Roshani, M.; Jahangir, M.; Gharib, A. Effective direct esterification of butanol by eco-friendly Preyssler catalyst, $[NaP_5W_{30}O_{110}]^{14}$. *J. Mol. Catal. A: Chem.* **2007**, *271*, 126–130.
54. Heravi, M.M.; Bakhtiari, K.; Bamoharram, F.F. An efficient and chemoselective synthesis of acylals from aromatic aldehydes and their regeneration, catalyzed by 12-molybdophosphoric acid. *Catal. Commun.* **2006**, *7*, 499–501.
55. Heravi, M.M.; Haghighi, M.; Derikvand, F.; Bamoharram, F.F. Efficient method for tetrahydropyranylation of alcohols and phenols and

deprotection of THP ethers using $H_{14}[NaP_5W_{30}O_{110}]$ as a green catalyst. *Synth. Commun.* **2006**, *36*, 3103–3107.

56. Heravi, M.M.; Bakhtiari, K.; Daroogheha, Z.; Bamoharram, F.F. An efficient synthesis of 2,4,6-triarylpyridines catalyzed by heteropolyacid under solvent-free conditions. *Catal. Commun.* **2007**, *8*, 1991–1994.
57. Heravi, M.M.; Sadjadi, S.; Oskooie, H.A.; Hekmatshoar, R.; Bamoharram, F.F. An efficient synthesis of 3H-1,5-benzodiazepine derivatives catalyzed by heteropolyacids as a heterogeneous recyclable catalyst. *J. Chin. Chem. Soc.* **2008**, *55*, 842–845.
58. Heravi, M.M.; Bakhtiari, K.; Daroogheha, Z.; Bamoharram, F.F. Facile heteropolyacid-promoted synthesis of 14-substituted-14-H-dibenzo[a,j] xanthene derivatives under solvent-free conditions. *J. Mol. Catal. A: Chem.* **2007**, *273*, 99–101.
59. Motamedi, R.; Heravi, M.M.; Bamoharram, F.F.; Haeri, A. Facile routes to 1,2,4-triazolo[3,4-b][1,3,4]thiadiazines and 1,2,4-triazino[3,4-b][1,3,4]thiadiazine by heteropolyacides. *J. Heterocycl. Chem.* **2008**, *45*, 1211–1214.
60. Heravi, M.M.; Zadsirjan, V.; Bakhtiari, K.; Oskooie, H.A.; Bamoharram, F.F. Green and reusable heteropolyacid catalyzed oxidation of benzylic, allylic and aliphatic alcohols to carbonyl compounds. *Catal. Commun.* **2007**, *8*, 315–318.
61. Heravi, M.M.; Benmorad, T.; Bakhtiari, K.; Bamoharram, F.F.; Oskooie, H.H. $H_{3+x}PMo_{12-x}V_xO_{40}$ (heteropolyacids)-catalyzed regioselective nitration of phenol to o-nitrophenol in heterogeneous system. *J. Mol. Catal. A: Chem.* **2007**, *264*, 318–321.
62. Heravi, M.M.; Ranjbar, L.; Derikvand, F.; Bamoharram, F.F. $H_6P_2W_{18}O_{62}$: An efficient and reusable catalyst for one-pot synthesis of [beta]-acetamido ketone and esters. *Catal. Commun.* **2007**, *8*, 289–291.
63. Heravi, M.M.; Behbahani, F.K.; Bamoharram, F.F. $H_{14}[NaP_5W_{30}O_{110}]$: A heteropoly acid catalyzed acetylation of alcohols and phenols in acetic anhydride. *J. Mol. Catal. A: Chem.* **2006**, *253*, 16–19.
64. Heravi, M.M.; Behbahani, F.K.; Oskooie, H.A.; Bamoharram, F.F. $H_{14}[NaP_5W_{29}MoO_{110}]$: a novel and useful catalyst for aminolysis of epoxides with amines under solvent-free conditions. *Chin. J. Chem.* **2008**, *26*, 2150–2154.
65. Hekmatshoar, R.; Sajadi, S.; Heravi, M.M.; Bamoharram, F.F. H-$_{14}[NaP_5W_{30}O_{110}]$ as a heterogeneous recyclable catalyst for the air oxidation of thiols under solvent free conditions. *Molecules* **2007**, *12*, 2223–2228A.
66. Heravi, M.M.; Derikvand, F.; Ranjbar, L.; Bamoharram, F.F. H-$_{14}[NaP_5W_{30}O_{110}]$ as a heterogeneous recyclable catalyst for the synthesis of 1,5-benzodiazepines in refluxing ethanol. *J. Mol. Catal. A–Chem.* **2007**, *261*, 156–159.
67. Oskooie, H.A.; Heravi, M.M.; Bakhtiari, K.; Zadsirjan, V.; Bamoharram, F.F. $H_{14}[NaP_5W_{30}O_{110}]$ as an efficient catalyst for the one-pot synthesis of alpha-amino nitriles. *Synlett*. **2006**, 1768–1770.
68. Heravi, M.M.; Javanmardi, N.; Oskooie, H.A.; Baghernejad, B.; Heidari, M.; Bamoharram, F.F. Heteropolyacid as a new, green and recyclable catalyst for the synthesis of 2-aryl benzoxazole under solvent-free conditions. *J. Chin. Chem. Soc.* **2009**, *56*, 589–593.
69. Heravi, M.M.; Sadjadi, S.; Oskooie, H.A.; Shoar, R.H.; Bamoharram, F.F. Heteropolyacids as green and reusable catalysts for the synthesis of 3,1,5-benzoxadiazepines. *Molecules* **2007**, *12*, 255–262.
70. Heravi, M.M.; Derikvand, F.; Haeri, A.; Oskooie, H.A.; Bamoharram, F.F. Heteropolyacids as green and reusable catalysts for the synthesis of isoxazole derivatives. *Synth. Commun.* **2008**, *38*, 135–140.
71. Heravi, M.M.; Sadjadi, S.; Oskooie, H.A.; Shoar, R.H.; Bamoharram, F.F. Heteropolyacids as heterogeneous and recyclable catalysts for the synthesis of benzimidazoles. *Catal. Commun.* **2008**, *9*, 504–507.
72. Sadjadi, S.; Heravi, M.M.; Haj, N.M.; Oskooie, H.A.; Shoar, R.H.; Bamoharram, F.F. Heteropolyacids in synthesis of benzoyl hydrazone derivatives. *Bull. Chem. Soc. Ethiopia* **2009**, *23*, 467–472.
73. Heravi, M.M.; Khorasani, M.; Derikvand, F.; Oskooie, H.A.; Bamoharram, F.F. Highly efficient synthesis of coumarin derivatives in the presence of $H_{14}[NaP_5W_{30}O_{110}]$ as a green and reusable catalyst. *Catal. Commun.* **2007**, *8*, 1886–1890.
74. Heravi, M.M.; Derikvand, F.; Bamoharram, F.F. Highly efficient, four-component one-pot synthesis of tetrasubstituted imidazoles using Keggin-type heteropolyacids as green and reusable catalysts. *J. Mol. Catal. A: Chem.* **2007**, *263*, 112–114.
75. Heravi, M.M.; Bakhtiari, K.; Javadi, N.M.; Bamoharram, F.F.; Saeedi, M.; Oskooie, H.A. $K_7[PW_{11}CoO_{40}]$-catalyzed one-pot synthesis of polyhydroquinoline derivatives via the Hantzsch three component condensation. *J. Mol. Catal. A: Chem.* **2007**, *264*, 50–52.
76. Oskooie, H.A.; Heravi, M.M.; Javadi, N.M.; Bakhtiari, K.; Bamoharram, F.F. $K_7[PW_{11}CoO_{40}]$: Efficient and ecofriendly catalyst for the enamination of beta-dicarbonyl compounds. *Synth. Commun.* **2008**, *38*, 2864–2869.
77. Heravi, M.M.; Sadjadi, S.; Hekmatshoar, R.; Oskooie, H.A.; Bamoharram, F. Keggin-type heteropolyacids-catalyzed one pot oxidation-trimerization of alcohols into 2,4,6-trisubstituted-1,3,5-trioxanes. *Iranian J. Chem. Chem. Eng. Int. Eng. Ed.* **2009**, *28*, 131–136.
78. Bamoharram, F.F.; Heravi, M.M.; Ardalan, T.; Ardalan, P. A kinetic study of the electron-transfer in the reaction of tribenzylchlorotin with $[CoW_{12}O_{40}]^5$. *Chin. Chem. Lett.* **2009**, *20*, 1005–1009.
79. Heravi, M.M.; Ranjbar, L.; Derikvand, F.; Bamoharram, F.F. A modified and green Dakin-West reaction: An efficient and convenient method for a one-pot synthesis of [beta]-acetamido carbonyl compounds. *J. Mol. Catal. A: Chem.* **2007**, *271*, 28–31.
80. Heravi, M.M.; Bakhtiari, K.; Bamoharram, F.F. 12-Molybdophosphoric acid: A recyclable catalyst for the synthesis of Biginelli-type 3,4-dihydropyrimidine-2(1H)-ones. *Catal. Commun.* **2006**, *7*, 373–376.
81. Hekmatshoar, R.; Sajadi, S.; Sadjadi, S.; Heravi, M.M.; Beheshtiha, Y.S.; Bamoharram, F.F. Multifunctional catalysis of heteropoly acid: one-pot synthesis of quinolines from nitroarene and various aldehydes in the presence of hydrazine. *J. Chin. Chem. Soc.* **2008**, *55*, 1195–1198.
82. Heravi, M.M.; Bakhtiari, K.; Benmorad, T.; Bamoharram, F.F.; Oskooie, H.A.; Tehrani, M.H. Nitration of aromatic compounds catalyzed by divanadium-substituted molybdophosphoric acid, $H_5[PMo_{10}V_2O_{40}]$. *Monatshefte Fur Chemie* **2007**, *138*, 449–452.
83. Alizadeh, M.H.; Razavi, H.; Bamoharram, F.F.; Hassanzadeh, M.K.; Khoshnavazi, R.; Zonoz, F.M. Novel catalytic acetylation of alcohols with Preyssler's anion, $[NaP_5Wa_{30}O_{110}]^{14-}$. *Kinet. Catal.* **2003**, *44*, 524–528.
84. Gharib, A.; Daneshtalab, M.; Scheeren, J.W.; Bamoharram, F.F.; Roshani, M.; Jahangir, M. Novel catalytic synthesis of 6,7-dimethoxyisatin with the use of heteropolyacids (HPAs) as acid solid catalyst. *Pol. J.Chem. Technol.* **2009**, *11*, 5–7.
85. Heravi, M.M.; Baghernejad, B.; Oskooie, H.A.; Bamoharram, F.F. A novel method for the synthesis of 1(2h)-phthalazinone derivatives using heteropolyacids as heterogeneous and recyclable catalysts. *Heterocycl. Commun.* **2008**, *14*, 375–384.
86. Heravi, M.M.; Sadjadi, S.; Mokhtari Haj, N. Oskooie, H.A.; Shoar, R.H.; Bamoharram, F.F. A novel multi-component synthesis of 4-arylaminoquinazolines. *Tetra. Lett.* **2009**, *50*, 943–945.
87. Bamoharram, F.F.; Roshani, M.; Alizadeh, M.H.; Razavi, H.; Moghayadi, M. Novel oxidation of aromatic aldehydes catalyzed by Preyssler's anion $[NaP_5W_{30}O_{110}]^{14-}$. *J. Brazilian Chem. Soc.* **2006**, *17*, 505–509.
88. Bamoharram, F.F.; Heravi, M.M.; Roshani, M.; Tavakoli, N. N-oxidation of pyridine carboxylic acids using hydrogen peroxide catalyzed by a green heteropolyacid catalyst: Preyssler's anion, $[NaP_5W_{30}O_{110}]^{14}$. *J. Mol. Catal. A: Chem.* **2006**, *252*, 219–225.
89. Oskooie, H.A.; Heravi, M.M.; Derikvand, F.; Khorasani, M.; Bamoharram, F.F. On water: An efficient Knoevenagel condensation using 12-tungstophosphoric acid as a reusable green catalyst. *Synth. Commun.* **2006**, *36*, 2819–2823.

90. Heravi, M.M.; Sadjadi, S.; Oskooie, H.A.; Hekmatshoar, R.; Bamoharram, F.F. The one-pot synthesis of 2,4,5-triaryl-imidazoles using heteropolyacids as heterogeneous and recyclable catalysts. *J. Chin. Chem. Soc.* **2008**, *55*, 1199–1203.
91. Heravi, M.M.; Sadjadi, S.; Oskooie, H.A.; Shoar, R.H.; Bamoharram, F.F. One-pot synthesis of 2-arylbenzoxazoles promoted by heteropolyacids. *J. Chin. Chem. Soc.* **2008**, *55*, 890–895.
92. Gharib, A.; Daneshtalab, M.; Scheeren, J.W.; Bamoharram, F.F.; Roshani, M.; Jahangir, M. One-pot synthesis of (S)-2-(6-methoxynaphtalen-2-yl) propanoic acid, (S)-Naproxen using Preyssler and Keggin-type heteropolyacids as green and reusable catalysts. *Pol. J. Chem. Tech.* **2009**, *11*, 8–14.
93. Heravi, M.M.; Derikvand, F.; Hassan-Pour, S.; Bakhtiari, K.; Bamoharram, F.F.; Oskooie, H.A. Oxidative aromatization of Hantzsch 1,4-dihydropyridines in the presence of mixed-addenda vanadomolybdophosphate heteropolyacid, $H_6PMo_9V_3O_{40}$. *Bioorg. Med. Chem. Lett.* **2007**, *17*, 3305–3309.
94. Alizadeh, M.H.; Razavi, H.; Bamoharram, F.F.; Daneshvar, K. The oxidative cleavage of carbon—tin bond catalyzed by heteropolyacids of molybdenum. *J. Mol. Catal. A: Chem.* **2003**, *206*, 89–93.
95. Bamoharram, F.F.; Heravi, M.M.; Roshani, M.; Jahangir, M.; Gharib, A. Preyssler catalyst, $[NaP_5W_{30}O_{110}]^{14-}$: A green, efficient and reusable catalyst for esterification of salicylic acid with aliphatic and benzylic alcohols. *Appl. Catal. A* **2006**, *302*, 42–47.
96. Heravi, M.M.; Bamoharram, F.F.; Rajabzadeh, G.; Seifi, N.; Khatami, M. Preyssler heteropolyacid $[NaP_5W_{30}O_{110}]^{14-}$, as a new, green and recyclable catalyst for the synthesis of [1,2,4]triazino[4,3-b][1,2,4,5]tetrazines. *J. Mol. Catal. A: Chem.* **2006**, *259*, 213–217.
97. Heravi, M.M.; Sadjadi, S.; Haj, N.M.; Oskooie, H.A.; Bamoharram, F.F. Role of various heteropolyacids in the reaction of 4-hydroxycoumarin, aldehydes and ethylcyanoacetate. *Catal. Commun.* **2009**, *10*, 1643–1646.
98. Heravi, M.M.; Bakhtiari, K.; Javadi, N.M.; Oskooie, H.A.; Bamoharram, F.F. Selective acetylation of alcohols and amines with ethyl acetate in the presence of $H_6[PMo_9V_3O_{40}]$ as the catalyst. *Monatshefte Fur Chemie* **2007**, *138*, 445–447.
99. Bamoharram, F.F.; Chamani, J.; Heravi, M.M.; Rajabi, O.; Roshani, M.; Karimi, N.; Heravi, O.M. Spectroscopic investigations of interactions of geteropolyacids with alpha-lactalbumin complexes. *Asian J. Chem.* **2009**, *21*, 3385–3394.
100. Heravi, M.M.; Ranjbar, L.; Derikvand, F.; Bamoharram, F.F. Sulfamic acid as a cost-effective catalyst instead of metal-containing acids for the one-pot synthesis of [beta]-acetamido ketones. *J. Mol. Catal. A: Chem.* **2007**, *276*, 226–229.
101. Heravi, M.M.; Sadjadi, S.; Oskooie, H.A.; Shoar, R.H.; Bamoharram, F.F. The synthesis of coumarin-3-carboxylic acids and 3-acetyl-coumarin derivatives using heteropolyacids as heterogeneous and recyclable catalysts. *Catal. Commun.* **2008**, *9*, 470–474.
102. Bakavoli, M.; Pirouzi, F.; Nikpour, M.; Bamoharram, F.; Davoodnia, A. Synthesis of new tetracyclic fused imidazole Dderivatives. *Heterocycl. Commun.* **2009**, *15*, 31–41.
103. Heravi, M.M.; Ranjbar, L.; Derikvand, F.; Alimadadi, B.; Oskooie, H.A.; Bamoharram, F.F. A three component one-pot procedure for the synthesis of [1,2,4]triazolo/benzimidazolo-quinazolinone derivatives in the presence of $H_6P_2W_{18}O_{62}$ center dot 18H(2)O as a green and reusable catalyst. *Mol. Div.* **2008**, *12*, 181–185.
104. Heravi, M.M.; Jani, B.A.; Derikvand, F.; Bamoharram, F.F.; Oskooie, H.A. Three component, one-pot synthesis of dihydropyrano[3,2-c]chromene derivatives in the presence of $H_6P_2W_{18}O_{62}\cdot 18H_2O$ as a green and recyclable catalyst. *Catal. Commun.* **2008**, *10*, 272–275.
105. Bamoharram, F.F. Vibrational spectra study of the interactions between Keggin heteropolyanions and amino acids. *Molecules* **2009**, *14*, 3214–3221.
106. Heravi, M.M.; Bakhtiari, K.; Bamoharram, F.F.; Tehrani, M.H. Wells-Dawson type heteropolyacid catalyzed synthesis of quinoxaline derivatives at room temperature. *Monatshefte Fur Chemie* **2007**, *138*, 465–467.
107. Heravi, M.M.; Sadjadi, S.; Sadjadi, S.; Oskooie, H.A.; Shoar, R.H.; Bamoharram, F.F. Supported Preyssler Nanoparticles in Synthesis of 1,3-Diaryl-5-spirohexahydropyrimidines. *J. Chin. Chem. Soc.* **2009**, *56*, 246–250.
108. Bamoharram, F.F. Mano-Preyssler heteropolyacid: a novel nanocatalyst for poly-condensation of benzyl alcohols. *Asian J. Chem.* **2011**, *23*, 177–179.
109. Bamoharram, F.F.; Heravi, M.M.; Heravi, M.M.; Meraji, M. Synthesis of silver nanoparticles in the presence of a green heteropolyacid, $H_{14}[NaP_5W_{30}O_{110}]$, and their catalytic activity for photodegradation of methylene blue and methyl orange. *Inter. J. Green Nanotech.: Phys. Chem.* **2009**, *1*, 26–31.
110. Bamoharram, F.F.; Daneshvar, K.; Golmakani, A. Controlled synthesis and characterization of magnetite nanoparticles obtained by glycothermal method. *Inter. J. Nanomanufacturing* **2010**, *5*, 245–253.
111. Bamoharram, F.F.; Heravi, M.M.; Roushani, M.; Toosi, M. Synthesis and characterization of silica-supported Preyssler nanoparticles and its catalytic activity for photodegradation of methyl orange. *Green Chem. Lett. Rev.* **2009**, *2*, 35–41.
112. Huang, M.; Tso, E.; Datye, A.K.; Prairie, M.R.; Stange, B.M. Removal of silver in photographic processing waste by TiO_2-based photocatalysis. *Environ. Sci. Technol.* **1996**, *30*, 3084–3088.
113. Troupis, A.; Gkika, E.; Hiskia, A.; Papaconstantinou, E. Photocatalytic reduction of metals using polyoxometallates: recovery of metals or synthesis of metal nanoparticles. *Comptes Rendus Chimie* **2006**, *9*, 851–857.
114. Ahmadi, T.S.; Wang, Z.I.; Green, T.C.; Henglein, A.; El Sayed, M. Shape-controlled synthesis of colloidal platinum nanoparticles. *Science* **1996**, *272*, 1924–1925.
115. Chou, K.S.; Ren, C.Y. Synthesis of nanosized silver particles by chemical reduction method. *Mater. Chem. Phys.* **2000**, *64*, 241–246.
116. Lee, P.C.; Meisel, D. Adsorption and surface-enhanced Raman of silver and gold sols. *Phys. Chem.* **1982**, *86*, 3391–3395.
117. Shirtcliffe, N.; Nickel, U.; Schneider, S. Reproducible preparation of silver sols with small particle size using borohydride reduction: For use as nuclei for preparation of larger particles. *Colloid Interface Sci.* **1999**, *211*, 122–129.
118. Sondi, I.; Goia, D.V.; Matijevic, E. Preparation of highly concentrated stable dispersions of uniform silver nanoparticles. *Colloid Interface Sci*. **2003**, *260*, 75–81.
119. Weinstock, I.A. Homogeneous-phase electron-transfer reactions of polyoxometalates. *Chem. Rev.* **1998**, *98*, 113–170.
120. Yamase, T. Photo- and electrochromism of polyoxometalates and related materials. *Chem. Rev.* **1998**, *98*, 307–325.
121. Hiskia, A.; Papaconstantinou, E. Photocatalytic oxidation of organic compounds by polyoxometalates of molybdenum and tungsten. Catalyst regeneration by dioxygen. *Inorg. Chem.* **1992**, *31*, 163–167.
122. Gkika, E.; Troupis, A.; Hiskia, A.; Papaconstantinou, E. Photocatalytic reduction of chromium and oxidation of organics by polyoxometalates. *Appl. Catal. B: Environ.* **2006**, *62*, 28–34.
123. Mandal, S.; Selvakannan, P.R.; Pasricha, R.; Sastry, M. Keggin ions as UV-switchable reducing agents in the synthesis of Au core-Ag shell nanoparticles. *J. Amer. Chem. Soc.* **2003**, *125*, 8440–8441.
124. Triantis, T.; Troupis, A.; Gkika, E.; Alexakos, G.; Boukos, N.; Papaconstantinou, E.; Hiskia, A. Photocatalytic synthesis of Se nanoparticles using polyoxometalates. *Catal. Today* **2009**, *144*, 2–6.
125. Mandal, S.; Das, A.; Srivastava, R.; Sastry, M. Keggin ion mediated synthesis of hydrophobized Pd nanoparticles for multifunctional catalysis. *Langmuir* **2005**, *21*, 2408–2413.
126. Troupis, A.; Triantis, T.; Hiskia, A.; Papaconstantinou, E.; Rate-redox-controlled size-selective synthesis of silver nanoparticles using polyoxometlates. *Eur. J. Inorg. Chem.* **2008**, 5579–5586.
127. Troupis, A.; Hiskia, A.; Papaconstantinou, E. Photocatalytic reduction-recovery of silver using polyoxometalates. *Appl. Catal. B: Environ.* **2003**, *42*, 305–315.

128. Shanmugam, S.; Viswanathan, B.; Varadarajan, T.K. A novel single step chemical route for noble metal nanoparticles embedded organic-inorganic composite films. *Mater. Chem. Phys.* **2006**, *95*, 51–55.
129. Mandal, S.; Rautaray, D.; Sastry, M. *$Ag^{(+)}$-Keggin Ion Colloidal Particles as Novel Templates for the Growth of Silver Nanoparticle Assemblies*; Royal Society of Chemistry, Cambridge, ROYAUME-UNI: Cambridge, England, **2003**.
130. Laurent, R.; Claire, C.-C.; Sébastien, S.; Isabelle, L. Photocatalytic reduction of Ag_2SO_4 by Dawson-derived sandwich complex. *Macromol. Symp.* **2008**, *270*, 117–122.
131. Yang, L.; Shen, Y.; Xie, A.; Zhang, B. Facile size-controlled synthesis of silver nanoparticles in UV-irradiated tungstosilicate acid solution. *J. Phys. Chem. C* **2007**, *111*, 5300–5308.
132. Zhang, G.; Keita, B.; Dolbecq, A.; Mialane, P.; Sécheresse, F.; Miserque, F.; Nadjo, L. Green chemistry-type one-step synthesis of silver nanostructures based on Mo^{V}-Mo^{VI} mixed-valence polyoxometalates. *Chem. Mater.* **2007**, *19*, 5821–5823.
133. Xu, M.; Liu, C.; Xu, Y.; Li, W.; Wu, L. Incorporation of metal nanoparticles into $H_3PMo_{12}O_{40}$ hybrid Langmuir-Blodgett film through in-situ reduction. *Colloids Surf., A* **2009**, *333*, 46–52.
134. Niu, C.; Wu, Y.; Wang, Z.; Li, Z.; Li, R. Synthesis and shapes of gold nanoparticles by using transition metal monosubstituted heteropolyanions as photocatalysts and stabilizers. *Front Chem. China* **2009**, *4*, 44–47.
135. Shankar, S.S.; Rai, A.; Ahmad, A.; Sastry, M. Controlling the optical properties of lemongrass extract synthesized gold nanotriangles and potential application in infrared-absorbing optical coatings. *Chem. Mater.* **2005**, *17*, 566–572.
136. Sarma, T.K.; Chattopadhyay, A. Starch-mediated shape-selective synthesis of Au nanoparticles with tunable longitudinal plasmon resonance. *Langmuir* **2004**, *20*, 3520–3524.
137. Zhang, G.; Keita, B.; Biboum, R.N.; Miserque, F.; Berthet, P.; Dolbecq, A.; Mialane, P.; Catala, L.; Nadjo, L. Synthesis of various crystalline gold nanostructures in water: the polyoxometalate β-$[H_4PMo_{12}O_{40}]^{3-}$ as the reducing and stabilizing agent. *Journal of Mater. Chem.* **2009**, *19*, 8639–8644.
138. Berger, L.I. *Semiconductor Materials*; CRC Press: Boca Raton, FL, **1997**.
139. Yang, L.B.; Shen, Y.H.; Xie, A.J.; Liang, J.J.; Zhang, B.C. Synthesis of Se nanoparticles by using TSA ion and its photocatalytic application for decolorization of cango red under UV irradiation. *Mater. Res. Bull.* **2008**, *43*, 572–582.
140. Murray, C.B.; Norris, D.J.; Bawendi, M.G. Synthesis and characterization of nearly monodisperse CdE (E = sulfur, selenium, tellurium) semiconductor nanocrystallites. *J. Amer. Chem. Soc.* **1993**, *115*, 8706–8715.
141. Wang, Y.; Herron, N. Nanometer-sized semiconductor clusters: materials synthesis, quantum size effects, and photophysical properties. *J. Phys. Chem.* **1991**, *95*, 525–532.
142. Zhang, B.; Shen, Y.; Xie, A.; Yang, L.; Wang, X. Shape controlled synthesis of CdS nanostructures in tungstosilicate acid solution by a novel approach. *Mater. Chem. Phys.* **2009**, *116*, 392–399.
143. Mandal, S.; Rautaray, D.; Sanyal, A.; Sastry, M. Synthesis and assembly of CdS nanoparticles in Keggin ion colloidal particles as templates. *Phys. Chem. B* **2004**, *108*, 7126–7131.
144. Shen, Y.; Xie, A.; Chen, Z.; Xu, W.; Yao, H.; Li, S.; Huang, L.; Wu, Z.; Kong, X. Controlled synthesis of calcium carbonate nanocrystals with multi-morphologies in different bicontinuous microemulsions. *Mater. Sci. Eng., A* **2007**, *443*, 95–100.
145. Rautaray, D.; Sainkar, R.S.; Sastry, M. *Ca^{2+}-Keggin Anion Colloidal Particles as Templates for the Growth of Star-Shaped Calcite Crystal Assemblies*; American Chemical Society: Washington, DC, **2003**.
146. Purcar, V.; Donescu, D.; Petcu, C.; Luque, R.; Macquarrie, D.J. Palladium metal nanoparticles on organically modified thin hybrid films. *Catal. Commun.* **2009**, *10*, 395–400.
147. Troupis, A.; Hiskia, A.; Papaconstantinou, E. Selective photocatalytic reduction-recovery of palladium using polyoxometallates. *Appl. Catal. B: Environ.* **2004**, *52*, 41–48.
148. Anne, D.; Jean-Daniel, C., Pierre, M.; Jérôme, M.; Francis, S.; Bineta, K.; Luis Roberto Brudna, H.; Frédéric, M.; Louis, N. Hexa- and dodecanuclear polyoxomolybdate cyclic compounds: application toward the facile synthesis of nanoparticles and film electrodeposition. *Chem. Eur. J.* **2009**, *15*, 733–741.
149. Zhang, J.; Keita, B.; Nadjo, L.; Mbomekalle, I.M.; Liu, T. Self-assembly of polyoxometalate macroanion-capped Pd^0 nanoparticles in aqueous solution. *Langmuir* **2008**, *24*, 5277–5283.